Multiomic interpretation of fungus-infected ant metabolomes during manipulated summit disease.

I. Will[1*], G.M. Attardo[2], C. de Bekker[1,3*]

1: University of Central Florida, Biology Department, USA

2: University of California – Davis, Entomology and Nematology Department, USA

3: Utrecht University, Biology Department, NL

* Corresponding authors: ian.will@knights.ucf.edu (IW), a.m.debekker@uu.nl (CdB)

ORCiD: 0000-0002-2396-6778 (IW), 0000-0001-6265-2969 (GMD), 0000-0002-7325-172X (CdB)

Abstract

Camponotus floridanus ants show altered behaviors followed by a fatal summiting phenotype when infected with manipulating *Ophiocordyceps camponoti-floridani* fungi. Host summiting as a strategy to increase transmission is also observed in parasite taxa beyond fungi, including aquatic and terrestrial helminths and baculoviruses. The drastic phenotypic changes observed likely reflect large physiological changes within host cells that span molecular levels from metabolites to nucleic acids. Nevertheless, the underlying mechanisms have not been fully characterized. To investigate the small molecules underlying summiting behavior, we infected *C. floridanus* ants with *O. camponoti-floridani* and sampled their heads for LC-MS/MS when we observed the characteristic manipulation phenotype. We link this metabolomic data with our previous genomic and transcriptomic data to propose mechanisms that underly manipulated summiting behavior in "zombie ants." This "multiomic" evidence points toward dysregulation of neurotransmitter levels and neuronal signaling. We propose that these processes are altered during infection and manipulation based on: 1) differential expression of neurotransmitter synthesis and receptor genes, 2) altered abundance of metabolites and neurotransmitters (precursors) with known behavioral effects in ants and other insects, and 3) possible suppression of a connected immunity pathway. We additionally report signals for fungal metabolic activity during manipulation and early evidence for alterations of host processes related to detoxification, anti-stress protectants, and insect hormone metabolism.

Introduction

Infections often leads to altered host phenotypes that can be adaptive for the host or parasite. Parasite-adaptive changes in animal host behavior are mostly referred to as manipulations. Apparent manipulations of host behavior and physiology occur in a broad range of host and parasite taxa. While descriptive examples are plenty, the underlying mechanisms are still in the process of being revealed (Thomas *et al.* 2010; Moore 2013; Heil 2016; Libersat *et al.* 2018; de Bekker *et al.* 2021).

The ant-manipulating *Ophiocordyceps* (zombie ant fungi) have been leveraged in laboratory studies to better understand the mechanistic basis of behavioral manipulation (de Bekker *et al.* 2014a, 2021; de Bekker 2019). Manipulated ants display summit disease: a common parasitic manipulation observed in invertebrates where the manipulated individual occupies an elevated location and dies in a stereotypical manner (Lovett *et al.* 2020; de Bekker *et al.* 2021). These final, elevated, exposed summit positions can be adaptive for the parasite by either aiding direct dispersal of infectious propagules or trophic transmission. In the case of *Ophiocordyceps*, ants latch and bite onto their final summit perches until their death, which is thought to promote development of the fungal fruiting body and dispersal of the spores therein (Andersen *et al.* 2009; Hughes *et al.* 2011; Loreto *et al.* 2018; Andriolli *et al.* 2019; Will *et al.* 2022b). Moreover, preceding this fatal change in behavior, infected ants also deviate from foraging trails and increase locomotor activity, reduce nestmate communication, and convulse (Pontoppidan *et al.* 2009; Andersen *et al.* 2009; Hughes *et al.* 2011; de Bekker *et al.* 2015; Sakolrak *et al.* 2018; Trinh *et al.* 2021)

These various changes may represent behaviors that can be easily coopted for manipulation by the fungal parasite (de Bekker *et al.* 2021). As such, the parasite may be taking advantage of existing host processes and symptoms without relying on costly mechanisms to “rewire” their hosts (Adamo 2019; Lovett *et al.* 2020). A deeper understanding of the fitness costs and benefits of these behaviors, for both the host and parasite, may reveal that some could also be adaptive for the host, at the individual or group level (perhaps especially so for eusocial animals, such as ants). Regardless of the ultimate “source” of the altered behaviors observed, physiological and molecular characterizations of hosts displaying modified

53 behavior may offer a glimpse into how parasites (or hosts) modulate animal behavior, the coevolution of
54 specialized host-parasite relationships, and undescribed properties of proteins and metabolites involved.
55 In the myrmecophilous *Ophiocordyceps*, investigations of phenotypes, genomes, transcriptomes,
56 and metabolomes continue to bring various mechanistic hypotheses of behavioral manipulation into
57 focus. The range of hypotheses touch upon: fungal neuromodulators and effector proteins, host circadian
58 rhythms and phototropism, insect hormones, fungal neuroprotectants, and ant muscular hyperactivity (de
59 Bekker *et al.* 2014a; Kobmoo *et al.* 2018; de Bekker 2019; Mangold *et al.* 2019; Zheng *et al.* 2019;
60 Loreto and Hughes 2019; Will *et al.* 2020; Trinh *et al.* 2021; de Bekker and Das 2022). Previous
61 metabolomic studies, centered on the *Ophiocordyceps kimflemingiae* zombie ant fungus and its host
62 *Camponotus castaneus*, have identified various metabolites associated with manipulation. These
63 metabolomic signals also varied in a species-specific manner, changing when either the parasite or host
64 was a exchanged for a different species (de Bekker *et al.* 2014b; Zheng *et al.* 2019; Loreto and Hughes
65 2019). However, these studies did not place the results within the context of other types of "omics" data.
66 Doing so would present the opportunity to distinguish the most robust lines of evidence from the more
67 stochastic signals that might differ across experimental conditions and setups.
68 Here, we present a "multiomic" approach by conducting a metabolomic analysis of *Camponotus*
69 *floridanus* (Florida carpenter ant) manipulated by *Ophiocordyceps camponoti-floridani* (Florida zombie
70 ant fungus) interpreted in the context of our previous transcriptomic and genomic data (Will *et al.* 2020).
71 To add to our existing transcriptomic data, we collected metabolomic data using three liquid
72 chromatography-tandem mass spectrometry (LC-MS/MS) protocols. Our study compares whole head
73 samples of healthy *C. floridanus* ants and ants manipulated by *O. camponoti-floridani*, allowing direct
74 comparison to Will *et al.* 2020 transcriptomic ant-head data. We primarily focused our interpretation and
75 discussion of the results on altered metabolic pathways that are supported by a combination of metabolite
76 and gene signals. This improves mechanistic interrogation as the key processes of manipulation could
77 involve specialized and general mechanisms, host and parasite effectors, and changes from the genetic to
78 chemical level. At the same time, combining multiple omics approaches and datasets allowed us to

79 identify consistent and robust signals for key biological processes.

80 To analyze our metabolomics data we also combined multiple statistical methods to reduce the
81 inherent bias that any given analysis introduces. Data that represent substantial biological changes are
82 more likely to be selected by multiple complementary tests. Our reporting, therefore, highlights
83 manipulation-associated metabolite features that were selected by multiple statistical methods. Whole
84 heads contain the chemical profiles of ant neural tissue, muscle, and hemolymph in addition to fungal
85 cells that all may contain metabolites of most interest (Hughes *et al.* 2011; de Bekker *et al.* 2014b, 2015;
86 Fredericksen *et al.* 2017; Mangold *et al.* 2019; Zheng *et al.* 2019; Loreto and Hughes 2019). As such, we
87 propose multiple pathways and compounds that reflect, or drive, manipulated behavior in *Ophiocordyceps*
88 infected ants.

89

90 **Results & discussion**

91 **Infection mortality, observations of manipulation, and LC-MS/MS datasets:** Similar to
92 previous laboratory infections with *O. camponoti-floridani* (Will *et al.* 2020), *C. floridani* displaying
93 manipulated biting in this study were collected between 4 hr before to 0.5 hr after dawn, beginning three
94 weeks after infection (Fig. 1). Sham treatment healthy ants showed no mortality until 29 days post
95 injection (dpi), whereas infection treatment ants began to die immediately once we started recording
96 deaths on 4 dpi. This difference in survival was markedly different between treatments ($p = 4.1E-7$, log-
97 rank test) (Fig. 1A). In total, three sham treatment ants died out of the 28 (11%) that survived through 3
98 dpi. Twenty-three infected ants were manipulated out of the 39 (59%) that survived through 3 dpi. The
99 other 16 infected ants died with visible blastospore loads but without observed behavioral manipulation.

100 In total, these experimental infections produced 20 manipulated ants, 20 healthy (sham) ants, and
101 three blank-collection samples produced from the ant housing of the sham treatment (Fig. 2A). From
102 these samples, we produced three LC-MS/MS datasets, “biogenic amines,” “polyphenols,” and “lipids,”
103 containing 2,955, 4,315, and 4,924 analyzed features, respectively. (Fig. 2A-B).

104

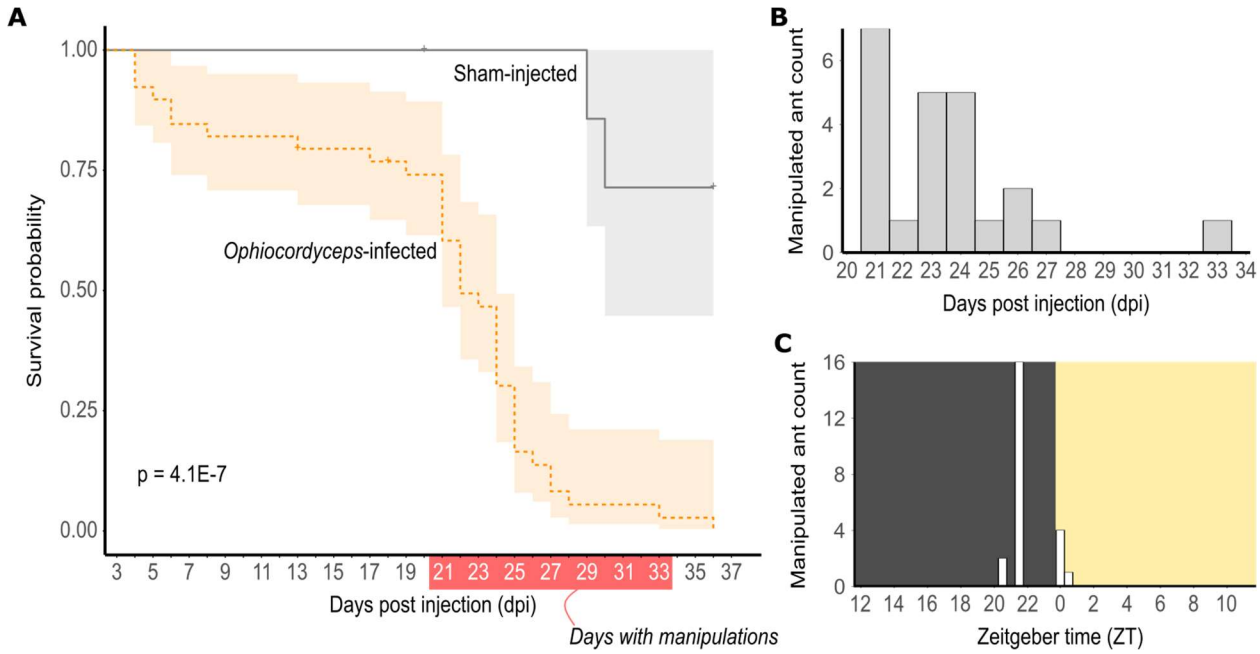

Figure 1. Ant manipulations occur at stereotypical days and times.
A) *O. camponoti-floridani* infection leads to significantly increased mortality compared to sham treatment (p = 4.1E-7, log-rank test). B) Manipulated ants most often appeared 21-27 dpi, but as late as 33 dpi. C) Manipulated ants were collected near dawn, most often at ZT 21.5, 2.5 hr before lights turned on.

Metabolomic feature selection and grouping for pathway enrichment analyses: After data quality control and filtering (Fig. 2B), we constructed a set of features for study-wide pathway enrichment analysis that distinguished healthy and manipulated ants by: categorization as differentially abundant metabolites (DAMs), loading values in principal component analyses (PCAs), and importance for navigating decision trees (Boruta) (Kursa and Rudnicki 2010) (Fig. 2C). Combining all three LC-MS/MS datasets, approximately 60% of features were DAMs, with most DAMs increasing in abundance in manipulated ants compared to healthy controls (Fig. 3A, Table 5). Separation of treatment groups by PCA only clearly clustered along PC1 (ca. 60% to 80%), with PC2 (ca. 4% to 9%) and other PCs (not shown) describing little of the variation between treatments (Fig. 3B). Using Boruta random forests, we found ca.

122 40% of features to be “confirmed” as “important” for distinguishing treatment types (Table 5). We

123 performed pathway analyses with a study-wide group of features that satisfied at least

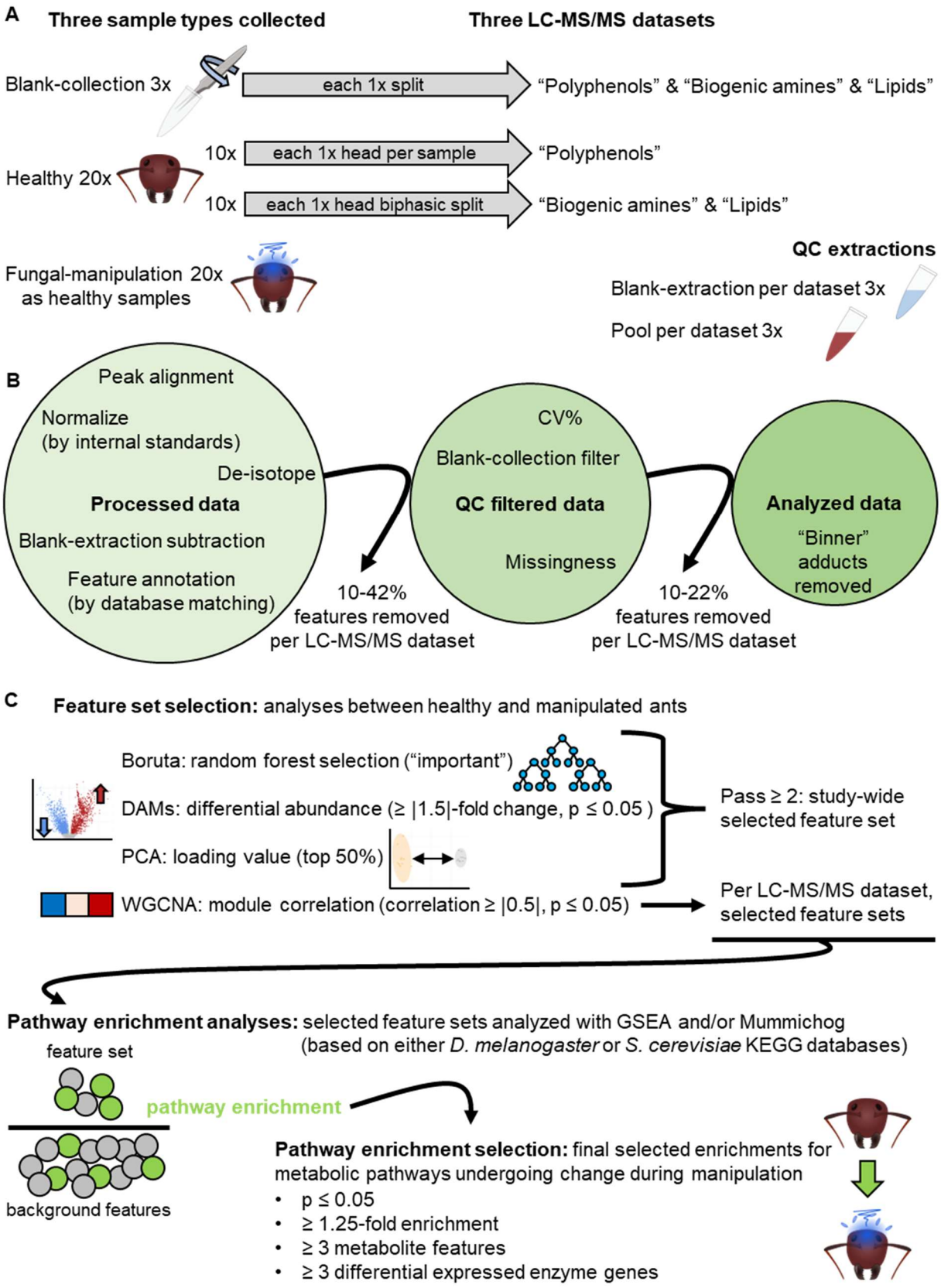

124 **Figure 2. Experimental overview and analytical framework for enrichment analyses.**

A) Three types of experimental samples were collected, blank-collections (mock sampling using tools and ant housing for healthy ants), healthy ants (given sham-injections only), and manipulated ants (infected with *Ophiocordyceps* and displaying manipulation phenotypes). The metabolomics core facility introduced two quality control (QC) extractions. First, blank-extractions using core facility materials only (and therefore distinct from experimental blank-collections). Second, pooled extractions of all samples used for a given LC-MS/MS dataset. Three LC-MS/MS datasets were produced, each being an untargeted analysis but tailored to different chemistries to collect broad data overall. B) The metabolomics core generated "Processed data" from which we produced "QC filtered data" and "Analyzed data" by applying quality control and data reduction steps. C) We used multiple statistical tests to select features of interest for metabolic pathway enrichment analyses. Results from those enrichment analyses were subsequently subjected to multiple filters to arrive at a final set of pathways and feature sets of interest. Full details on these samples and approaches are given in Methods.

two of following criteria: (*i*) it was a DAM, (*ii*) it was among the highest 50% of absolute PC1 loading values, or (*iii*) it was confirmed by Boruta. Most features that satisfied at least two requirements (n = 6,468 features, 53% of a total 12,194 features), in fact satisfied all three (n = 4,656, 72% of features passing two criteria) (Fig. 2C, 15C, Supp. Table 1, Supp. Data 1). The feature set passing at least two filters contained 347 of the 760 (46%) features given compound annotations by the WCMC. The many features passing our filters is likely due to a combination of metabolites related specifically to infection processes and general aspects of fungal metabolism, as *O. camponti-floridani* cells were only present in manipulated ants. For this set of features passing at least two selection filters, we jointly analyzed them with Mummichog and a gene set enrichment analysis (GSEA)-based approach in MetaboAnalyst for enriched metabolic pathways found in the Kyoto Encyclopedia of Genes and Genomes (KEGG) (Fig. 2C) (Kanehisa and Goto 2000; Li *et al.* 2013; Pang *et al.* 2021). We detected eight significantly enriched pathways that passed our p-value, minimum metabolite feature, fold-enrichment, and enzyme differentially expressed gene (DEG) thresholds (Fig. 2C, Table 6, Supp. Data 2). These enzyme DEGs use previously published expression data from an *Ophiocordyceps* manipulation study (Will *et al.* 2020) and were associated here with their respective KEGG metabolic pathways. Most enzyme DEGs were downregulated both in the ant (90%) and the fungus (62%). This degree of downregulation is higher than previously found for transcriptome-wide DEGs during manipulation (Will *et al.* 2020) (Supp. File 1).

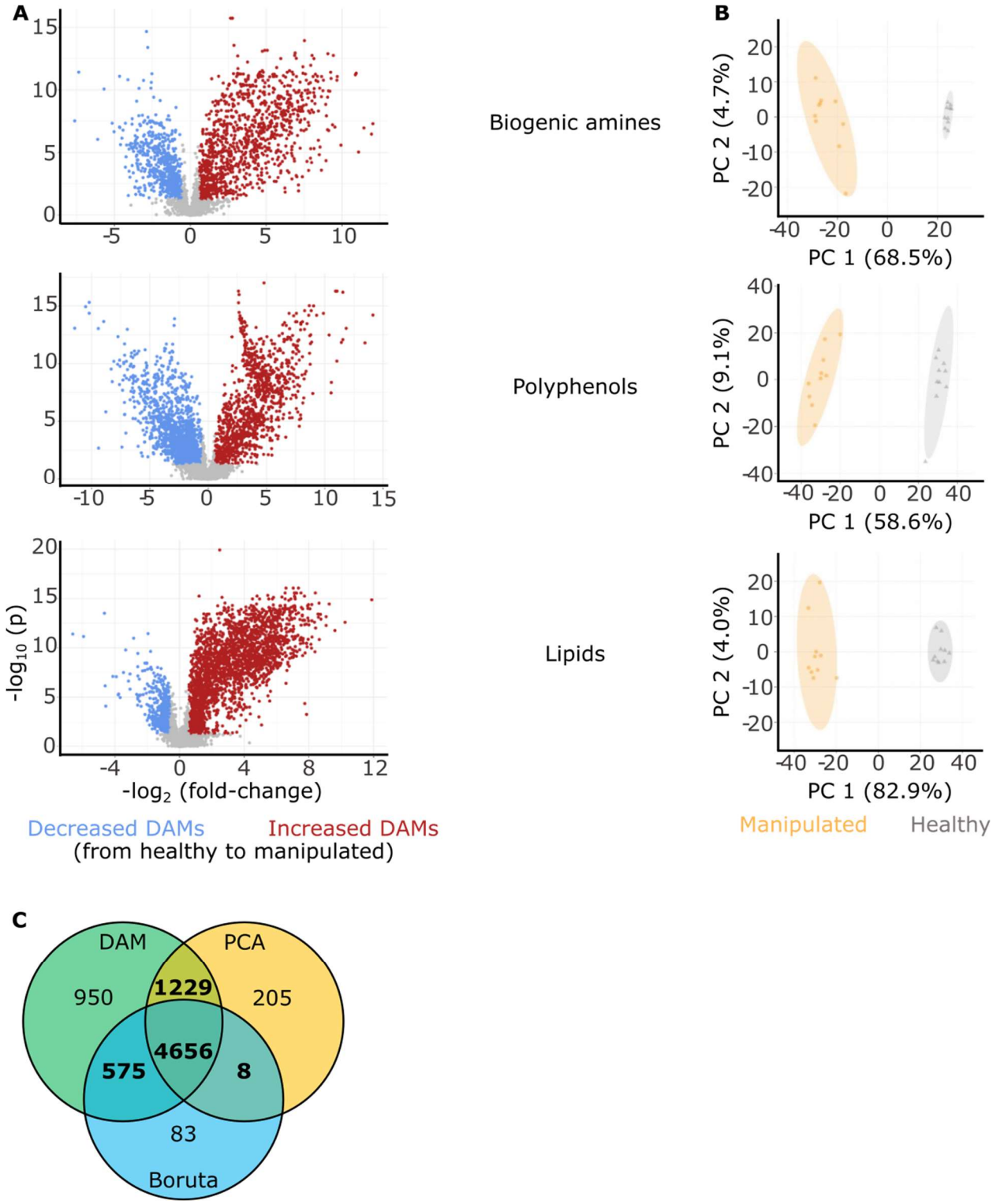

Figure 3. Feature selection overview.

A) Volcano plots per dataset show DAMs that increased (red) or decreased (blue) at manipulation according to a 1.5-

158 fold change and $p \leq 0.05$. B) PCAs for each dataset show distinct clustering of samples between manipulated (orange)
159 and healthy ants (gray) along PC1. C) Features that passed at least two selection criteria (bold) were used for study-
160 wide pathway analyses. We used DAM analyses to select features as described above, PCAs to select features in the
161 top 50% of PC 1 loading values, and the Boruta analysis to select features identified as "important."
162
163 **Table 1. All enriched KEGG pathways selected across analyzed feature sets.**
164 KEGG pathways that were found in Mummichog or GSEA analyses ($p \leq 0.05$) also were required to show a
165 minimum 1.25-fold enrichment, three features contributing to that enrichment, and three DEGs that were
166 homologous to representative enzyme genes within that pathway. Each pathway is listed alphabetically once in the
167 table, with all feature sets (network modules or the study-wide feature set that passed at least two selection filters)
168 that were enriched for that pathway.

Enriched KEGG metabolic pathway	**Feature sets**					
Alanine, aspartate and glutamate metabolism	P13					
Amino sugar and nucleotide sugar metabolism	A1	P1	P2	P3	P18	study-wide
Aminoacyl-tRNA biosynthesis	L3	P2	P11			
Arginine and proline metabolism	A1	P2				
Arginine biosynthesis	A1					
Ascorbate and aldarate metabolism	A1	P13				
beta-Alanine metabolism	P2	study-wide				
Biosynthesis of unsaturated fatty acids	L2	L10	P3	study-wide		
Butanoate metabolism	P2					
Citrate cycle (TCA cycle)	P3	P13				
Cyanoamino acid metabolism	A1					
Cysteine and methionine metabolism	L1	P1	P18			
Drug metabolism - cytochrome P450	L3	P3				
Drug metabolism - other enzymes	A1	study-wide				
Fatty acid degradation	P3					
Folate biosynthesis	P2					
Fructose and mannose metabolism	P2	P18				
Galactose metabolism	A1	P18	study-wide			
Glutathione metabolism	A1					
Glycerolipid metabolism	P2					
Glycerophospholipid metabolism	P2	study-wide				
Glycine, serine and threonine metabolism	P2	P11				
Glycolysis or Gluconeogenesis	P3					
Glyoxylate and dicarboxylate metabolism	P13					
Histidine metabolism	A1					

Inositol phosphate metabolism	P2					
Insect hormone biosynthesis	A1	P3				
Lysine biosynthesis	A1					
Lysine degradation	P2					
Metabolism of xenobiotics by cytochrome P450	A1	P2				
Nicotinate and nicotinamide metabolism	P2					
Pantothenate and CoA biosynthesis	A1	P18				
Pentose and glucuronate interconversions	A1	P18				
Pentose phosphate pathway	A1	L1	P1	P2	P3	P18
Phenylalanine metabolism	A1	P2				
Purine metabolism	L1	P1	P18			
Pyrimidine metabolism	A1	P11	study-wide			
Pyruvate metabolism	P13					
Starch and sucrose metabolism	A1	P3	P18			
Sulfur metabolism	P2					
Taurine and hypotaurine metabolism	L1	P1				
Tyrosine metabolism	P2	P3				
Ubiquinone and other terpenoid-quinone biosynthesis	P3					
Valine, leucine and isoleucine degradation	P18	study-wide				

Many metabolite features in our dataset were uniquely represented in manipulated samples: 454 features were never detected in healthy sham treatment ants and 1,781 additional features either were detected in less than 50% of the healthy ants and/or their median peak value was not at least double that of blank-collection controls (2,235 features total). These features may represent compounds tightly regulated and scarce in the healthy ant or uniquely produced by the fungus. We predicted that this feature set might have been enriched for hallmarks of infection and manipulation processes. However, no significant pathway enrichments were returned from our Mummichog and GSEA analyses. This could indicate that these metabolites are not linked by common metabolic pathways and/or many of these metabolites were not well annotated in the KEGG databases (e.g., species-specific metabolites).

We used a weighted gene co-expression network analysis (WGNCA) based approach to cluster metabolite features that similarly change abundance levels between healthy and manipulated *C. floridanus* treatments (Fig. 2C) (Langfelder and Horvath 2008). Co-expression (or co-abundance)

182 networks, in some cases, suggest linked biological functions and activity in the same metabolic processes
183 (Stuart *et al.* 2003; Carlson *et al.* 2006; Gillis and Pavlidis 2012; Bartzis *et al.* 2017). We detected three
184 biogenic amine, eight polyphenol, and five lipid network modules that were significantly correlated to
185 treatment (Fig. 4). A total of six biogenic amine (A1-A6), 19 polyphenol (P1-P19), and 10 lipid (L1-L10)
186 networks were created in total. Due to our sparse annotation

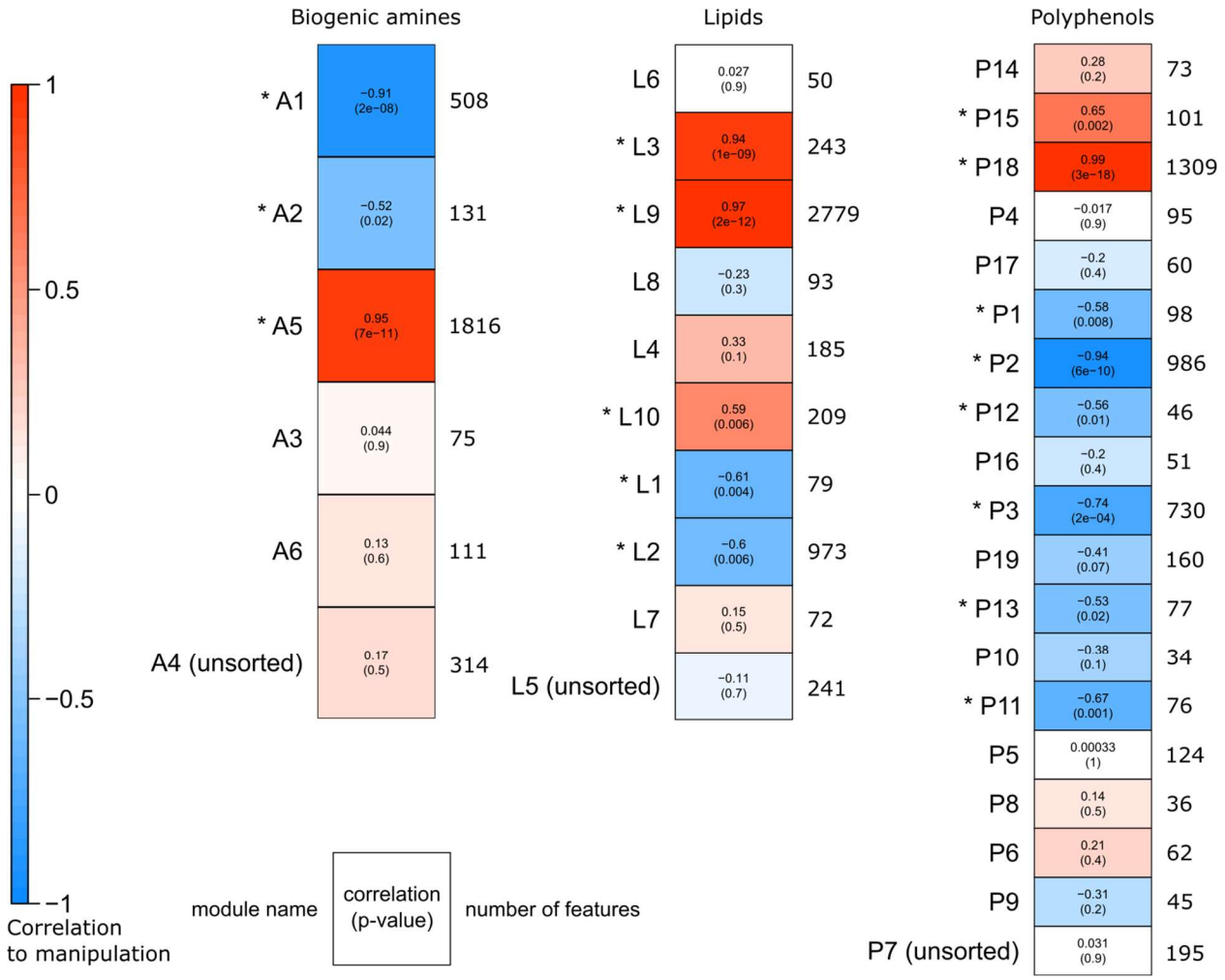

187

188 **Figure 4. WGCNA network modules of metabolite features and their correlation to manipulation.**
189 In total we detected three, five, and eight significantly correlated (Student correlation ≥ |0.5|, $p \leq 0.05$, denoted with
190 *) network modules to manipulation in the biogenic amines, lipids, and polyphenol datasets, respectively. Network
191 modules were constructed as unsigned, meaning the direction of the correlation describes the network as a whole,
192 although some features may be anti-correlated within the module. "Unsorted" modules contain all features that were
193 not successfully correlated to other features in a network (i.e., by default labeled "gray" by R package WGCNA).
194

195 data, we were not able to consistently compare hub features. As such, we considered all available
196 annotations within a network module and Mummichog pathway enrichments (Fig. 2C). Across all
197 network modules significantly correlated to the transition from healthy to manipulated ants, 44 unique
198 enriched KEGG pathways were selected, which included the eight found across the study-wide data that
199 passed at least two selection filters (Table 6, Supp. Data 2).

200 **The biogenic monoamine neurotransmitters dopamine, serotonin, and octopamine are**
201 **known to modulate ant activity and may be proximate drivers of diseased behaviors:** A combination
202 of pathway enrichments, annotated DAMs, and DEGs suggest that shifts in metabolism associated with
203 neurotransmitters relate to behavioral alterations in *C. floridanus* infected and manipulated by *O.*
204 *camponoti-floridani*. The monoamine neurotransmitters dopamine, serotonin, and octopamine (analogous
205 to vertebrate norepinephrine) have been implicated in modulating locomotor, foraging, learning, social,
206 reproductive, and aggressive behaviors in many insects, and have been tested in social insects, including
207 ants (Adamo 2008; Aonuma and Watanabe 2012; Adamo *et al.* 2013; Kamhi *et al.* 2017; Verlinden
208 2018). Serotonin, octopamine, and melanin derived from L-3,4-dihydroxyphenylalanine (L-DOPA), or
209 tyrosine and dopamine, have roles in insect immunity as well (Geun *et al.* 2009; González-Santoyo and
210 Córdoba-Aguilar 2012). Administration of dopamine and serotonin to *Formica polyctena* wood ants or
211 *Odontomachus kuroiwae* trap-jaw ants have produced altered behaviors in the laboratory, such as
212 aggressive mandible-opening or biting behaviors and defensive responses (Szczuka *et al.* 2013; Aonuma
213 2020). In the field, *Pogonomyrmex barbatus* harvester ant dopamine levels positively correlated with
214 foraging trips, as seen both by dopamine supplementation and inhibition (Friedman *et al.* 2018).
215 Similarly, pharmacological depletion of serotonin led to reduced and impaired trail-following foraging
216 behavior in *Pheidole dentata* ants (Muscedere *et al.* 2012). In *Formica aquilonia*, there is evidence for
217 octopamine increasing aggressive behaviors (Yakovlev 2018), however, clear signs of increased
218 aggression with octopamine treatment was not found in *F. polyctena* (Szczuka *et al.* 2013). Octopamine
219 additionally appears to modulate the social behavior of trophallaxis in *Camponotus fellah*, while serotonin
220 had no significant effect (Boulay *et al.* 2000). As such, the exact effects of these neurotransmitters can

221 differ by species and social or physiological context. However, many of these affected behaviors are
222 relatable to the disease phenotypes observed in *Ophicordyceps* infected ants. Observations of
223 *Ophiocordyceps*-infected ants include changes in behavior leading to increased walking, deviation from
224 foraging trails, reduced nestmate communication, and the final manipulated bite (Pontoppidan *et al.* 2009;
225 Andersen *et al.* 2009; Hughes *et al.* 2011; de Bekker *et al.* 2015; Trinh *et al.* 2021).

226 Furthermore, gene expression networks negatively correlated between the ant and fungus were
227 enriched for host neuronal function and parasite manipulation-associated secreted proteins. This
228 correlation suggested parasite effectors promote, directly or indirectly, the downregulation of host gene
229 modules related to neuronal maintenance, circadian rhythm, olfaction, and memory (Will *et al.* 2020).
230 Additionally, direct host-parasite interactions have been hypothesized to occur by fungal proteins binding
231 ant neuroreceptors for dopamine, serotonin, and octopamine (Will *et al.* 2022a preprint). Although we did
232 not directly identify dopamine, serotonin, or octopamine in our metabolomic data, we did measure
233 features annotated as biosynthetically related compounds.

234 *Changes in dopamine metabolism possibly modified ant behaviors and shifted host-pathogen*
235 *immunological interactions during manipulation.* A combination of metabolomic and transcriptomic data
236 indirectly suggest increased dopamine metabolism in manipulated ants. The metabolomic signals
237 consisted of changes in neurotransmitter precursor abundances and enrichment of pathways in metabolite
238 network modules correlated to manipulation. Phenylalanine and tyrosine are precursors in synthesis
239 pathways for dopamine and octopamine. KEGG pathway "phenylalanine metabolism" was enriched in
240 both network modules A1 and P2 ($p = 0.026$ and 0.028, fold-enrichment = 1.5 and 1.9, respectively), both
241 of which were negatively correlated to manipulated ant samples. Additionally, KEGG pathway "tyrosine
242 metabolism" was enriched in modules P2 and P3 ($p = 0.030$ and 0.024, fold-enrichment = 1.4 and 1.6,
243 respectively), both also negatively correlated to manipulation. Moreover, module P2 also contained the
244 most informative compound annotations regarding dopamine metabolism.

245 The immediate precursor to dopamine, L-DOPA, was 2.8-fold reduced in abundance in
246 manipulated ants ($p = 0.008$, and in the top-50% of PC1) (Fig. 5). L-tyrosine was also annotated in

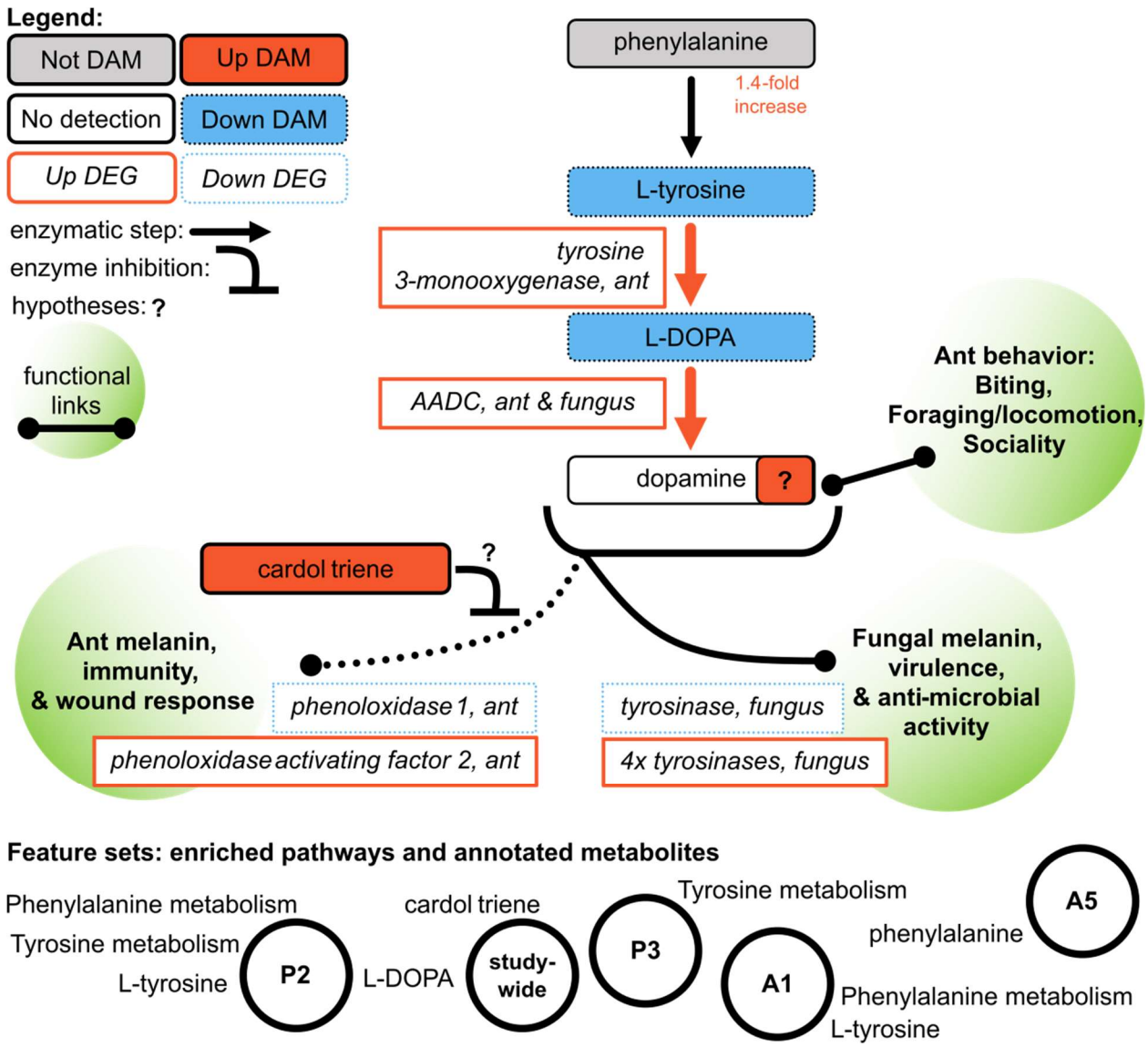

Figure 5. Altered neurotransmitter precursor metabolism suggests suppressed ant immunity, increased dopamine and serotonin, and reduced octopamine during infection and manipulation. Cardol triene may produced by the fungus to suppress ant immunity and thereby also increase availability of tyrosine and L-DOPA for dopamine synthesis. L-amino acid decarboxylase (AADC) catalyzes the final step of dopamine and serotonin synthesis and is upregulated by manipulated ants. A reduction of L-DOPA and tryptophan suggest that these compounds are being converted into dopamine and serotonin, respectively. Upregulation of an ant kynurenine aminotransferase possibly increases or maintains (if the kynurenine precursor is reduced) kynurenic acid levels. The possible of reduction of octopamine concentration follows the reasoning that it requires L-tyrosine for its synthesis, which is reduced during manipulation, and there is no compensatory upregulation of enzyme genes in the octopamine pathway to compete with upregulated dopamine biosynthesis. Dysregulated ant behavior during infection and manipulation may arise due to this altered neurotransmitter metabolism. Network modules from which

discussed feature annotations or enriched pathways reside are given at the bottom of the figure. Increases are indicated by solid lines and red color, decreases by dotted lines and blue color, metabolites are in rounded rectangles, genes are in rectangles, annotated metabolites that were not DAMs have gray color, compounds with white color were not identified in the LC-MS/MS data, and hypothesized functional links are given in the shaded circles. Metabolic steps that did not have DEG are shown as black arrows when useful for context but are omitted elsewhere. A squiggled arrow indicates metabolite interaction with a receptor. Tryptophan is given colored as a reduced abundance DAM, but was selected rather by the Boruta analysis only and not the differential abundance t-test.

module P2 and is the precursor to L-DOPA and tyramine. The latter can be converted into the neurotransmitter octopamine. L-Tyrosine was a DAM with a 2.1-fold decrease in abundance ($p = 1E-4$, and Boruta confirmed). An annotation for tyrosine was also present in the network module A1, however, we did not identify this metabolite feature as a DAM ($p = 0.154$, 1.2-fold reduction). Outside of network modules A1, P2, and P3, we also detected phenylalanine, the precursor to tyrosine. Phenylalanine showed a modest increase in abundance during manipulation just below our 1.5-fold change threshold for classification as a DAM ($p = 0.019$, 1.4-fold increase) (Fig. 5). Decreases in L-tyrosine and L-DOPA could be difficult to interpret alone, however in combination with RNAseq data, we found evidence for increased dopamine synthesis that offers one explanation for the depletion of these dopamine precursors.

During manipulation, both ant hosts and fungal parasites upregulated an aromatic L-amino acid decarboxylase (AADC) gene (Fig. 5). This enzyme catalyzes the final step of L-DOPA conversion to dopamine and the conversion of L-5-hydroxytryptophan to serotonin (Dakshinamurti *et al.* 2017). The AADC enzyme requires vitamin B6 as a cofactor and we detected differential abundance of an inactive vitamer form and a precursor for *de novo* synthesis in module A5 (Supp. File 2). However, the combination of metabolomic and transcriptomic data available do not provide for a clear interpretation for if active vitamin B6 is changing in abundance and in which organism(s).

A tyrosine 3-monooxygenase, which catalyzes the rate-limiting conversion of L-tyrosine to L-DOPA, was upregulated by manipulated ants. Meanwhile, the ant homolog to Henna (i.e., DTPHu phenylalanine 4-monooxygenase), which converts phenylalanine to L-tyrosine was not differentially

287 expressed. This enzyme also converts peripheral tryptophan to the serotonin precursor in *D. melanogaster*
288 (Neckameyer and White 1992; Coleman and Neckameyer 2005; Neckameyer *et al.* 2007). This consistent
289 expression may help explain the only modest change of phenylalanine during manipulation while its
290 derivatives were found at lower concentrations.

291 Dopamine and its precursors can also be converted into melanin, a key compound for insect
292 wound response and immunity (González-Santoyo and Córdoba-Aguilar 2012; Sugumaran and Barek
293 2016; Wang *et al.* 2017). Fungi can also synthesize melanin for use in host-pathogen interactions and
294 against competing microbes (Nosanchuk and Casadevall 2006; Nosanchuk *et al.* 2015). We found
295 evidence that this pathway for melanin production is reduced in the ant during manipulation and,
296 possibly, increased in the fungus (Fig. 5).

297 We propose that the production of a fungal-derived compound may inhibit tyrosinases necessary
298 to convert dopamine-pathway metabolites to melanin and hence simultaneously steer these metabolites
299 toward dopamine production. This metabolite feature was annotated as cardol triene (i.e., 5-(8,11,14-
300 pentadecatrienyl)resorcinol) and was a DAM only detected in manipulated ant samples ($p = 0.0073$,
301 median peak value = 19,604, in the top 50% of PC1) (Fig. 5). As cardol triene was never detected in
302 healthy ants, it plausibly is produced solely by the fungus, although we cannot discount the possibility
303 that production of this metabolite is produced by ants combatting infection and completely absent in
304 healthy individuals. We detected the putative cardol triene in six of 10 manipulation samples, this could
305 indicate that cardol triene levels are tightly regulated. Cardol triene has been shown to inhibit tyrosinase
306 oxidation of L-DOPA (Zhuang *et al.* 2010). In insects, phenoloxidases are a type of tyrosinase and are
307 key enzymes that begin the conversion of dopamine and L-DOPA to pro-immune melanin production
308 pathways (Gorman and Arakane 2010; González-Santoyo and Córdoba-Aguilar 2012; Wang *et al.* 2017).
309 As such, we hypothesize that fungal cardol triene chemically inhibits host phenoloxidase activity to
310 reduce melanin metabolism.

311 Additionally, ants showed mixed transcriptional signals related to the melanin-immune response
312 by phenoloxidase and phenoloxidase activating factor genes (Fig. 5) (Piao *et al.* 2005). Entomopathogen

313 infections suppress phenoloxidase activity in mosquitoes and the inhibition of activation of pro-
314 phenoloxidase has been hypothesized as a mechanism of fungal interference with insect host immunity
315 (Feng *et al.* 2015; Ramirez *et al.* 2018). In addition to suppressing host melanin production, the fungus
316 may be converting L-DOPA or related compounds into fungal melanin precursors, as four upregulated
317 and one downregulated tyrosinases were found during manipulation (Fig. 5). Three of the upregulated
318 fungal tyrosinases are putatively secreted and may possibly interact with host tyrosine and its derivatives.
319 The sum result of this proposed altered dopamine metabolism could weaken host immunity, bolster
320 parasite pathogenicity, and drive altered host behavior by increased dopamine concentration (Fig. 5).
321 *Serotonin and octopamine metabolism may also correlate to manipulated ant behavior.*
322 Biosynthetically and phenotypically intertwined with dopamine, fluctuating serotonin and octopamine
323 concentrations may contribute to manipulated ant behavior. Although the metabolomic signals for these
324 compounds were less robust than for dopamine, we found multiomic evidence that offers support for
325 hypotheses of increasing serotonin and decreasing octopamine (Supp. File 3). For example, upregulation
326 of the AADC enzyme shared between dopamine and serotonin pathways and at least one signal for the
327 reduction of tryptophan (selected by Boruta), which can be converted into the precursor for serotonin.
328 Coupled with the increasing serotonin, we additionally propose a hypothesis for increased kynueric acid,
329 which is also tied to tryptophan and may act as a neuroprotectant for heavily diseased and manipulated
330 ants (Supp. File 3).
331 *Multiomic synthesis of transcriptomic and metabolomic data.* Our hypotheses link enzyme gene
332 transcription and metabolite precursor abundance to predict an increase of dopamine with a reduction in
333 host melanin and immunity. Using similar reasoning, but with less robust metabolomic support, we
334 consider increases of serotonin and kynurenic acid, while octopamine may be reduced (Supp. File 3). An
335 alternative interpretation of the data could be that increased gene expression does not indicate elevated,
336 functional protein abundance in every case, and may even be a homeostatic response to low enzyme
337 activity or substrate abundance. However, without new proteomic data, we suggest that inferring protein
338 levels by transcription to generally be the most parsimonious explanation. Similarly, reduced precursor

339 abundances could reflect wide-spread reduced levels of metabolites, including neurotransmitter products.
340 But in the context of the observed behavioral manipulation phenotypes and reconciling transcriptomic and
341 metabolomic data, we propose a set of hypotheses we deem most plausible. Regardless of whether each
342 neurotransmitter discussed is increased or decreased in abundance, our data link changes in
343 neuromodulatory processes and parasitically manipulated behavior.

344 **Altered glycerophospholipid metabolism suggested increased fungal cell membrane activity**
345 **and ant accumulation of the excitatory neurotransmitter, acetylcholine:** The KEGG pathway
346 "glycerophospholipid metabolism" was enriched in module P2 and in study-wide features passing at least
347 two selection filters (p =0.024 and 0.030, fold-enrichment = 1.9 and 1.4, respectively). We found
348 evidence for two possible major effects, changes in cell membrane composition and the accumulation of
349 acetylcholine. Of our annotated features, metabolic signals centered on choline offered the most insight
350 into altered glycerophospholipid metabolism. Glycerophospholipids and choline-containing compounds
351 have been associated with neurodegenerative disease, such as Alzheimer's or Parkinson's, and insect
352 host-pathogen responses (Walter *et al.* 2004; Hoxmeier *et al.* 2015; Alecu and Bennett 2019). Choline is a
353 key component involved in the synthesis of phospholipids associated with forming cell membranes,
354 especially as incorporated through phosphatidylcholine (Li and Vance 2008). Although, in fungi and
355 insects, phosphatidylethanolamine is also a major cell membrane component (Batrakov *et al.* 2001;
356 Dawaliby *et al.* 2016; Cassilly and Reynolds 2018). Using the lipids LC-MS/MS dataset we compared
357 peak values of phosphatidylethanolamines (n = 95 features) and phosphatidylcholines (n = 85 features)
358 and found phosphatidylethanolamines to indeed be abundant in our insect and fungal tissue samples.
359 Within healthy ants, phosphatidylethanolamines were only slightly more abundant (1.10-fold greater)
360 than phosphatidylcholines (t-test, p = 0.017, t = -2.657). Within fungus-manipulated ants, there was no
361 strong difference (t-test, p = 0.739, t = -0.339, phosphatidylethanolamines 1.05-fold higher). As both
362 phospholipid types were nearly equally abundant, we considered changes of metabolites of either class
363 could reflect important processes during manipulation.

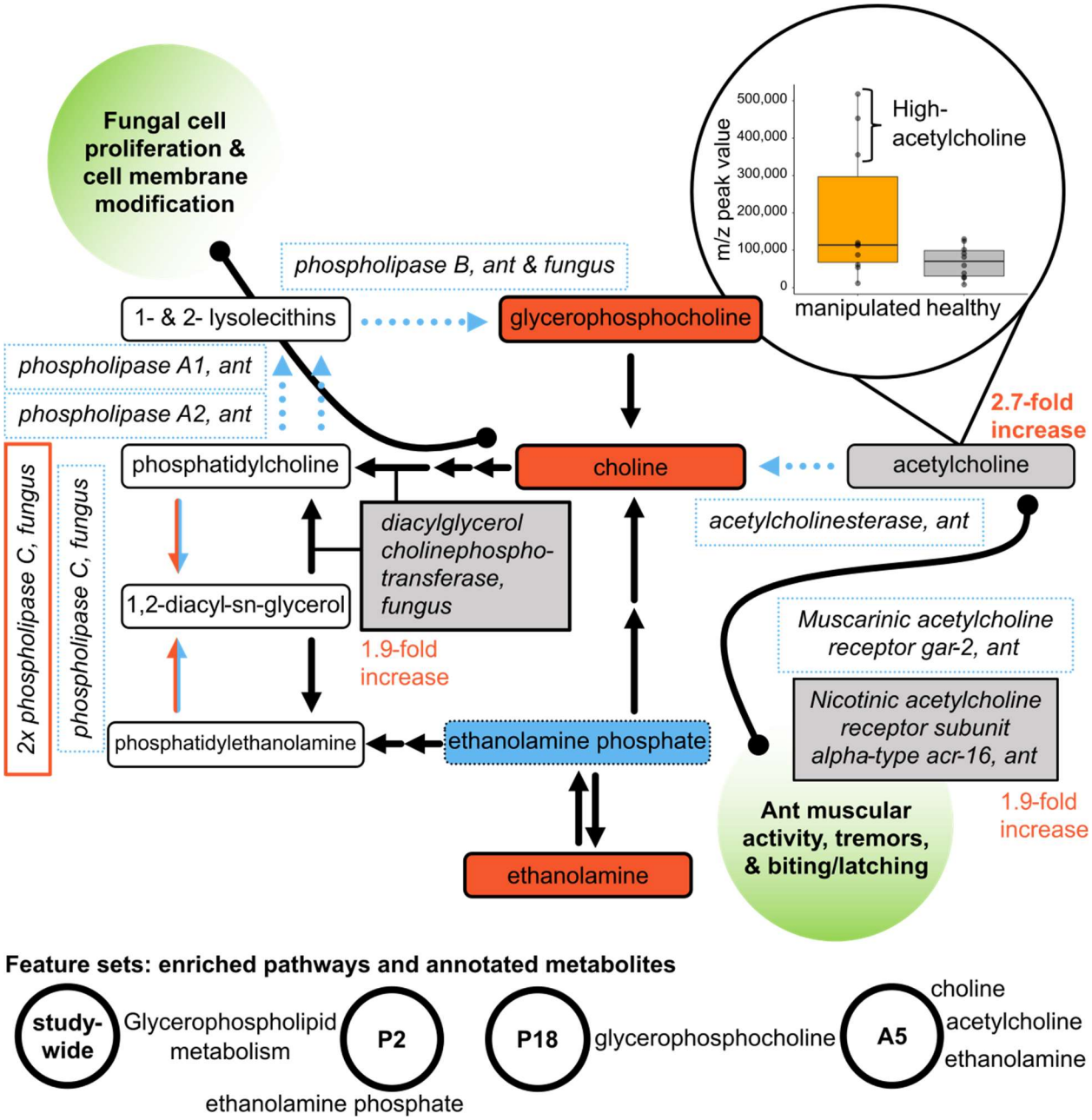

Figure 6. Changing glycerophospholipid metabolism during manipulation primarily indicate altered acetylcholine levels in the ant and cell membrane metabolism in the fungus.

Manipulated ant samples appeared to have two distinct groups, one with high acetylcholine and one with levels similar to healthy ants. In manipulated ants, the putative acetylcholinesterase and two acetylcholine receptor genes were downregulated, suggesting acetylcholine levels were accumulating. We hypothesize that increased acetylcholine in manipulated ants is associated with the increased muscular activity during early manipulation (e.g., tremors, biting, and latching behavior). Once the ant is secured in a summited position and the mandible muscles (and associated neurons) are further degraded, the fungus may be scavenging and converting the available acetylcholine to choline, thereby rapidly reducing acetylcholine levels. The fungus may be converting choline to

374 phospholipids, such as phosphatidylcholine to remodel and build cell membranes. Although we did detect multiple
375 features in the class of phosphatidylcholines and phosphatidylethanolamines, we did not identify the singular
376 metabolites "phosphatidylcholine" and "phosphatidylethanolamine" themselves. Network modules from which
377 discussed feature annotations or enriched pathways reside are given at the bottom of the figure. Increases are
378 indicated by solid lines and red color, decreases by dotted lines and blue color, metabolites are in rounded
379 rectangles, genes are in rectangles, annotated metabolites or genes that were not DAMs or DEGs have gray color,
380 compounds with white color were not identified in the LC-MS/MS data, and hypothesized functional links are given
381 in the shaded circles. Metabolic steps that did not have DEG are shown as black arrows when useful for context but
382 are omitted elsewhere. A squiggled arrow indicates metabolite interaction with a receptor.
383

384 Choline was a DAM increasing during manipulation (p = 1.7E-11, 20.0-fold increase, passing all
385 selection criteria) (Fig. 6). We also observed other DAMs related to choline within the
386 glycerophospholipid metabolism pathway. Glycerophosphocholine, a choline precursor was increased at
387 manipulation and detected in two datasets (p = 3.4E-11 and 1.2E-7, 5.9- and 7.7-fold increase, passing all
388 three selection criteria). We also detected two DAMs interconnected between choline and
389 phosphatidylethanolamine: ethanolamine (p = 5.2E-5, 2.1-fold increase, also Boruta confirmed) and
390 ethanolamine phosphate (p =1.6E-9, 5.5-fold decrease, passing all selection criteria) (Fig. 6). Three
391 putative *Ophiocordyceps* phospholipase C genes were DEGs, two upregulated and one downregulated
392 (Fig. 6). Broadly, phospholipid C proteins cleave phospholipids and have been implicated in cell
393 signaling, pathogenicity, and cell membrane metabolism (Pokotylo *et al.* 2013). When cleaving either
394 phosphatidylcholine or phosphatidylethanolamine they can produce an intermediate 1,2-diacyl-sn-
395 glycerol product. Additionally, the fungus expressed a putative diacylglycerol cholinephosphotransferase
396 gene 1.9-fold higher during manipulation, nearly qualifying as a DEG. This enzyme combines 1,2-diacyl-
397 sn-glycerol and CDP-choline to produce phosphatidylcholine. Phosphatidylcholine could then be
398 converted to glycerophosphocholine within two metabolic steps, but this pathway appeared to be
399 downregulated. Three genes putatively encoding the enzymes driving this conversion were downregulated
400 in the ant (phospholipases A1, A2, and B). In the fungus, a phospholipase B-like gene was also
401 downregulated (Fig. 6). The net effect appears to be fungal composition and/or catabolism of

402 phosphatidylethanolamines and synthesis of phosphatidylcholines leading to a minor compositional shift
403 overall during manipulation - but perhaps including specific and important changes we cannot yet identify
404 (Fig. 6). Modification of the cell membrane could be necessary to accommodate transmembrane proteins
405 or secretory activity involving organelle membranes such as in the endoplasmic reticulum (van der Veen
406 *et al.* 2017; Shyu *et al.* 2019).

407 Choline can also be metabolized into acetylcholine, the most abundant excitatory
408 neurotransmitter in insects (Gauthier 2010). In bees, excessive activation of acetylcholine receptors can
409 cause changes in locomotor, navigational, foraging, and social behaviors (Grünewald and Siefert 2019).
410 Acetylcholine can be rapidly converted back to choline by the activity of the acetylcholinesterase enzyme,
411 which has been a target of enzyme-inhibiting insecticides (Quinn 1987; Fournier *et al.* 1992; Colovic *et*
412 *al.* 2013; Singh *et al.* 2017). From this fast enzymatic activity, we intuit that acetylcholine levels could
413 reflect changes in physiology and behavior at a fine timescale. A subgroup of the manipulated ant
414 samples showed markedly higher acetylcholine levels than both healthy and other manipulated ants (Fig.
415 6). As such, we propose a scenario of transiently increased acetylcholine during manipulation, only
416 detected in a subset of our samples.

417 Acetylcholine showed a 2.7-fold mean increase at manipulation overall, but was not identified as
418 a DAM ($p = 0.142$), with a feature-peak value distribution showing two distinct groups. Three
419 manipulated ants had 5.5-fold higher acetylcholine peak values than the other seven that spanned a similar
420 range as control samples (Fig. 6). Speculatively, this could indicate that, for some fast-changing
421 metabolites such as acetylcholine, our sampling approach captured multiple subtly different physiological
422 states during the dynamic process of behavioral manipulation. The previously collected transcriptomics
423 data similarly showed the broadest distribution of acetylcholinesterase-2 expression during manipulation.
424 In the ant, an acetylcholinesterase-2-like gene was downregulated during active manipulation overall, but
425 two of the five samples had 2.5-fold lower acetylcholinesterase expression than the other three (Supp. Fig.
426 1) (Will *et al.* 2020). As the ant dies, acetylcholinesterase-2 expression begins to rebound toward healthy
427 ant levels. Notably, acetylcholinesterase-2 is the functionally dominant acetylcholinesterase enzyme in

428 *Camponotus* and many hymenopterans (Kim and Lee 2013). Additionally, the ant downregulated a
429 putative muscarinic acetylcholine receptor gar 2 that has been found in sensory and motor neurons of *C.*
430 *elegans* (Lee *et al.* 2000). Nearly a DEG as well, a putative ant nicotinic acetylcholine receptor acr-16
431 subunit gene was expressed 1.9-fold lower during manipulation. Possibly, receptor downregulation
432 represents a homeostatic response to the proposed elevated acetylcholine levels present during part of
433 manipulated summiting and biting.

434 Although acetylcholine has fast-acting regulatory effects on motor behavior, importantly,
435 glutamate is the direct primary excitatory neurotransmitter at insect neuromuscular junctions (Johansen *et*
436 *al.* 1989; Gauthier 2010; Pflüger and Duch 2011). Glutamate was nearly classified as a reduced DAM (p
437 = 0.007, 1.4-fold decrease) while a related compound, glutamine, did qualify (p = 1.8E-6 and 6.2E-11,
438 3.3- and 3.8-fold decrease, in network module A5 and also P2, respectively), with transcriptomic
439 evidence that suggested the host and parasite may be mounting contrasting regulatory responses (Will *et*
440 *al.* 2020) (Supp. File 4).

441 **Common metabolites between *Ophiocordyceps*-*Camponotus* manipulations in two species**
442 **pairings:** Previous metabolomic studies with *O. kimflemingiae* have identified many metabolites
443 associated with infection of *C. castaneus* and proposed links between these compounds and manipulation
444 (de Bekker *et al.* 2014b; Zheng *et al.* 2019; Loreto and Hughes 2019). Laboratory co-culture of *O.*
445 *kimflemingiae* with brains from *C. castaneus* and other ant species showed shared metabolites and distinct
446 compounds reflecting a combination of target host-specific fungal secretions and ant species profile (de
447 Bekker *et al.* 2014b). Other studies have compared *O. kimflemingiae* infections to that by a generalist
448 entomopathogenic fungus, again finding both overlap and differences in metabolomic profiles (Zheng *et*
449 *al.* 2019; Loreto and Hughes 2019).

450 Ergothioneine, an amino acid produced by some fungi, but not animals, has been detected in
451 mixed ant-fungal tissue from manipulated ant brains and muscles (Zheng *et al.* 2019; Loreto and Hughes
452 2019). Corroborating these findings, we detected two ergothioneine signals (biogenic amine and
453 polyphenol datasets) that were wholly absent in the healthy ants or with peak values near that of blank-

454 collection samples (p = 7.3E-15 and 4.6E-12, passing all selection criteria). In addition to fungal
455 metabolism, ergothioneine has been discussed as a possible neuroprotectant to preserve the ant brain until
456 manipulated summiting and biting are complete (Loreto and Hughes 2019). Supporting this line of
457 reasoning, ergothioneine in the ant brain was not detected at elevated levels in moribund ants infected by
458 the generalist entomopathogen *Cordyceps bassiana* that consumes hosts more quickly, without inducing
459 summit disease, and appears to occupy the ant head capsule to a lesser extent than *Ophiocordyceps*
460 (Fredericksen *et al.* 2017; Loreto and Hughes 2019).

461 Previous work with *O. kimflemingiae* and this work with *O. camponoti-floridani* have found
462 adenosine and adenosine-phosphate (AMP) to be differentially abundant between manipulation and
463 healthy and/or generalist-infected ants (Zheng *et al.* 2019; Loreto and Hughes 2019). We found two
464 features annotated as adenosine, one which was not differentially abundant and one that was a reduced
465 DAM in manipulated samples (p = 6.6E-4, 2.5-fold decrease). In contrast, previous works found
466 adenosine to increase in abundance in both manipulated ant brains and mandible muscles (Zheng *et al.*
467 2019; Loreto and Hughes 2019). Whether these contrasting results indicate species-specific patterns or
468 high variation is unclear. We also found decreased AMP (p = 0.003, 2.1-decrease, Boruta confirmed) in
469 the head, as was found in manipulated *C. castaneus* (Zheng *et al.* 2019; Loreto and Hughes 2019). In *O.*
470 *kimflemingiae* infection, a role for adenosine mediated neuromodulation was hypothesized, as was
471 changing AMP levels possibly reflecting changes in mitochondrial activity (Zheng *et al.* 2019; Loreto and
472 Hughes 2019). Cyclic AMP is involved in many pathways, including as a secondary messenger in G-
473 protein coupled receptor signaling, which includes receptors for dopamine and other neurotransmitters,
474 and have been hypothesized to be implicated in manipulation based on gene expression and host-parasite
475 protein-protein interaction predictions (Will *et al.* 2020, 2022a preprint). If changing abundance of AMP
476 reflects upon the cyclic form as well, this could relate to dysregulation of receptor signaling.
477 Metabolically related to adenosine, hypoxanthine and inosine were also proposed to have links to
478 energetic and neurological processes in manipulated ants (Zheng *et al.* 2019; Loreto and Hughes 2019).
479 As in those studies, we also detected increased levels of hypoxanthine during manipulation, two of three

480 features annotated as hypoxanthine increased at manipulation (p = 0.007 and 7.7E-6, 1.6-fold increase or
481 absent in sham, the latter of which passed all selection criteria). We also detected one inosine and two
482 inosine-monophosphate features increased in manipulated ants (p = 0.002, 3.8E-7, and 1.4E-5, 1.9-, 2.8-,
483 2.5-fold increase, all Boruta confirmed). This could indicate the conversion of AMP and adenosine to
484 hypoxanthine primarily via inosine intermediates.

485 **Pathways and compounds with reduced multiomic support:** Metabolomics results without
486 robust multiomic support or clearly annotated metabolite features provide a basis for future investigations.
487 Pathway enrichments without high-confidence metabolite annotations suggested possible changes in
488 insect hormone and detoxification metabolism during manipulation (Supp. File 5). With supporting
489 metabolite annotations but lacking strong genomic or transcriptomic evidence, we speculate that the
490 fungus may synthesize a cytoprotectant (carnosine), which could be derived from host compounds and
491 protect key host tissues (e.g., brain) during infection (Supp. File 5).
492

493 **Conclusion**

494 Infection and behavioral manipulation of hosts could involve many interacting molecular and
495 cellular processes. As these host-parasite interactions are better characterized, we can also gain insights
496 into specialist co-evolutions, the mechanistic basis of animal behavior, and the discovery of new bioactive
497 compounds. To unravel the mechanistic complexity of infection and manipulated host behavior, we
498 require functional tests built upon robust hypotheses. Towards this goal, we studied parasitic
499 manipulation of *C. floridanus* by *O. camponoti-floridani*, combining metabolomic, transcriptomic, and
500 genomic data to develop a set of hypotheses regarding molecular processes during manipulation.

501 We found evidence for altered biogenic monoamine neurotransmitter production during infection
502 and manipulation that may be proximate causes of manipulated behavior. In total, we propose a scenario
503 where the manipulated ant has elevated production of dopamine, with possible increases of serotonin and
504 decreases of octopamine. The fungus may also simultaneously suppress the host's melanin and immunity
505 pathways while metabolizing dopamine and its precursors for fungal melanin production. Ants infected

506 by *Ophiocordyceps* display enhanced locomotion/activity levels, reduction of social behaviors, and a final
507 summit latching behavior – elements of these behaviors have already been associated with
508 neurotransmitter signaling in ants. Intriguingly, aquatic gammarid crustaceans manipulated by
509 acanthocephalan worms display a phototactic summiting and clinging phenotype in the water column
510 sometimes associated with increased serotonin, decreased octopamine, and suppressed phenoloxidase-
511 mediated immunity – essentially, parts of the same pattern we propose in manipulated *Camponotus*
512 (Helluy and Holmes 1990; Lefèvre *et al.* 2009; Helluy 2013; Herbison 2017). Manipulators of vertebrate
513 behavior may also leverage serotoninergic and dopaminergic processes to alter fish and mouse behaviors
514 related to escape responses, locomotion, and aggression (Shaw *et al.* 2009; Prandovszky *et al.* 2011;
515 Adamo *et al.* 2013; Lafferty and Shaw 2013). How much of the alteration of neurotransmitter metabolism
516 may be a general response to fungal infection and how much results from specific manipulation by
517 *Ophiocordyceps* is difficult to pinpoint at this time. However, cardol triene appears to be a fungal derived
518 compound that could suppress ant immunity and increase substrate availability for dopamine production.
519 Also, *Ophiocordyceps* upregulated three putatively secreted tyrosinases that possibly interact with host
520 dopamine/melanin precursors. Although less typically reported than their intracellular counterparts,
521 extracellular fungal tyrosinases have also been found in another fungus (Selinheimo *et al.* 2006;
522 Gasparetti *et al.* 2012). Dopamine, serotonin, and octopamine receptors appear to be directly targeted by
523 secreted fungal effector proteins as well (Will *et al.* 2022a preprint). Given the importance this may place
524 on a functional host brain and body, indications in our data for altered neuro/cyto-protectant
525 concentrations and detoxification metabolism may indeed reflect key changes in the manipulated
526 metabolome. Although, further evidence is required to fully assess this.
527 Changing glycerophospholipid metabolism during manipulation, largely centered on choline,
528 suggested fungal biosynthesis of cell membrane components and dysregulation of acetylcholine levels in
529 the ant. *Ophiocordyceps* may require increased choline-derived cell-membrane components used during
530 cell proliferation and membrane remodeling for structures such as lipid rafts or transmembrane proteins
531 important during infection and manipulation. Manipulated ants reduced expression of

532 acetylcholinesterase, and three metabolomic manipulation samples had notably higher acetylcholine
533 concentrations than the rest. Speculatively, transient high acetylcholine could contribute to summiting and
534 wandering behavior (i.e., increased locomotion), tremors, and the hypercontracted biting that locks
535 manipulated ants into place.

536 By inducing changes in neurotransmitters that regulate behavior in healthy ants, the fungus may
537 be impinging upon existing host systems to modify behavior rather than forcibly introducing novel
538 pathways. Indeed, many of the hallmark phenotypes of infection by ant-manipulating *Ophiocordyceps* are
539 not so dissimilar from activities influenced by levels of dopamine, serotonin, octopamine, and
540 acetylcholine in eusocial insects: foraging/locomotor behavior (i.e., summiting and hyperactivity),
541 sociality (i.e., wandering and reduced communication), and the biting/aggression (the final "death grip"
542 bite). Changes in social behavior could not only be a symptom of disease, but contribute to it as well. As
543 socially isolated infected ants may less frequently exchange trophallactic fluid with nestmates, these
544 infected individuals would lose an important source of nutrition, communication, and hormones (Leboeuf
545 *et al.* 2016) that may alter their metabolome. How exactly the fungus dysregulates physiological pathways
546 that influence behavior (e.g., juvenile hormone metabolism) and to what degree some level of
547 dysregulation is typical in many diseases is still unclear. These hypotheses can be further investigated by
548 functional tests (e.g., gene knockouts or dosing ants with metabolites) and LC-MS/MS validations of key
549 compounds using chemical standards.

550

551 **Methods**

552 **Ant collection & husbandry:** We used a single laboratory-housed wild-caught colony of *C.*
553 *floridanus* to produce all samples. This colony was collected in March 2021 in the University of Central
554 Florida arboretum. This colony had several hundred individuals including minors, majors, and brood.
555 Based on methods in Will *et al.* 2020, we housed the colony in a plastic container within a climate-
556 controlled incubator (I36VL, Percival) cycling 12 h-12 h, light-dark, 28 C°-20 C°, 65% RH-80% RH
557 daily cycles. Climate conditions cycled in a ramping manner, with a 4 h ramp from lights-on to a 4 h hold

558 at peak day conditions to a 4 h ramp to lights-off (additional husbandry details in Supp. File 6).

559 **Fungal strain OJ2.1 collection, culture, and storage:** *O. camponoti-floridani* strain OJ2.1 was
560 used to infect all ants in this work. We isolated this fungal strain using mycelium extracted from the
561 abdomen of a fresh, manipulated *C. floridanus* cadaver. This cadaver was found in the Ocala National
562 Forest, FL (29° 13' 41.7" N, 81° 41' 44.9" W). The isolation procedure, short ribosomal subunit genetic
563 validation, and culturing followed the protocols detailed in Will *et al.* 2020. In preparation for
564 experimental infections, we grew fungal cells for 10 days in liquid shaking cultures with Grace's medium
565 (Gibco) supplemented to 2.5% fetal bovine serum (Gibco) ("GF" medium). We then filtered (two-layers
566 of 12-ply gauze, Curity) and adjusted the blastospore cells to a working concentration of approximately 3
567 x 10^6 cells/mL (optical density 660 nm = ca. 0.5) prior to injection.

568 We have not incorporated isolated *in vitro* fungal control samples as was done for transcriptomic
569 analysis in Will *et al.* 2020. Such samples would not likely have been effective and efficient to include
570 given the higher number of samples required for robust LC-MS/MS analysis, fungal metabolite
571 production can be highly reflective of culture conditions (VanderMolen *et al.* 2013), and, unlike
572 transcriptomic analyses, we would not be able to discern the origin of metabolites in mixed-organism
573 manipulated ant samples regardless. Instead, we used the transcriptomic data to propose links of altered
574 metabolite abundances during manipulation to either the host or parasite.

575 **Experimental infections of ants:** Ten days before infection, we separated ants from their colony
576 into boxes per treatment group. For the *Ophiocordyceps*-infection treatment, we gathered 41 ants and 10
577 additional caretaker ants with painted abdomens (Testors paint), which did not receive the treatment but
578 assisted the 41 injected ants with recovery. One day before infection treatments, we removed the sugar
579 and water from the ant box to reduce the amount of fluid in the ants and ease the injection procedure. Due
580 to a husbandry accident that led to widespread death of the initial sham-infection treatment ants, we
581 repeated the sham treatment two weeks after the *Ophiocordyceps* experimental treatment. Ants from the
582 same colony were used for the sham treatment (n = 30 with 8 painted caretakers) and were maintained in
583 the same incubator as all other ants.

584 Ants were either anesthetized by placing their plastic box on top of ice prior to injection, or
585 directly injected at room temperature. We injected each ant with 0.5 µL *Ophiocordyceps* blastospores
586 (infection, n = 41) or 0.5 µL of GF (sham, n = 30) as detailed in Will *et al.* 2020. We placed the treated
587 ants and their painted caretaker ants in plaster-lined boxes with biting structures (*Tillandsia usneoides* tied
588 to wooden sticks with twine) and returned them to the climate-controlled incubator.

589 **Observation and sample collection for LC-MS/MS:** After 3 dpi we removed dead ants. Then,
590 we began screening for manipulated ants and deaths twice per day, at zeitgeber-time (ZT)-0, the
591 beginning of subjective day, and ZT-6, the mid-point of subjective day. At 10 dpi, we removed the
592 painted caretaker ants as previous work has observed *C. floridanus* to destroy and interfere with
593 manipulated nestmates, presumably as a component of their social immunity and nest hygiene (Diez *et al.*
594 2014; Will *et al.* 2020; Trinh *et al.* 2021). Starting 15 dpi, we began more frequent opportunistic checks
595 as behavioral manipulations of *C. floridanus* had been observed starting 19 dpi in the laboratory (Will *et*
596 *al.* 2020). After discovering the first manipulation at 21 dpi, we made multiple daily checks beginning at
597 ZT-20 and ending at ZT-14 (on the next subjective day). Previous laboratory *O. camponoti-floridani*
598 manipulations synchronized to the ants' subjective pre-dawn hours and we selected our observation times
599 to improve the odds of collecting manipulations close to their beginning (Will *et al.* 2020). We screened
600 non-manipulated mortalities for fungal infection by crushing tissue from the dead ant in 50 µL of water,
601 briefly touchdown centrifuging, and examining 15 µL of the supernatant on a microscope. Notable levels
602 of fungal cells were always and only seen in the *Ophiocordyceps* treatment ants. We analyzed and plotted
603 survival data using the R packages survival and survminer in R (v 4.1) with R Studio (v. 2021.09.2)
604 (RStudio Team 2015; Therneau 2015; Kassambara *et al.* 2019; R Core Team 2021).

605 *LC-MS/MS samples.* We collected live manipulated ants displaying characteristic summiting
606 biting behavior for LC-MS/MS immediately upon discovery (n = 20) (Fig. 2A). We subsequently
607 collected dpi-matched sham ants at ZT-21.5, as this was the most common time at which manipulated
608 ants were collected (n = 20) (see Results and Discussion, Fig. 2A). Manipulated ants found after death
609 were recorded for survival statistics but not used in the LC-MS/MS analyses (n = 3). For manipulated ant

610 collection, we clipped the biting substrate just above and below the manipulated ant and submerged the
611 ant in liquid nitrogen briefly until frozen. The sample was then placed in a pre-chilled, sterile 2 mL
612 microcentrifuge tube (USA Scientific) kept in liquid nitrogen until long-term storage at -80 C°. We
613 collected sham ant samples in a similar manner, plucked from the experiment box with forceps.

614 We created three blank-collection samples at the beginning, middle, and end of manipulated ant
615 sampling, i.e., after the first, 10th, and 20th manipulated ants were found (n = 3) (Fig. 2A). We made
616 blank-collection samples by briefly touching the forceps to the floor of the sham treatment housing boxes,
617 submerging them in liquid nitrogen, and swirling them in a microcentrifuge tube. We cleaned all tools and
618 surfaces with 70% ethanol and deionized water before sampling and between sample types.

619 We later prepared collected samples for LC-MS/MS by isolating ant heads. Each frozen ant was
620 quickly processed on a plastic petri dish (USA Scientific) on a bed of dry ice. Using forceps, we removed
621 biting substrate from the ant's mandibles if needed, snapped the head off, and placed it in a new
622 microcentrifuge tube. Heads were paired together by collection date into 10 two-head pools per treatment,
623 but later separated for analysis (see below). For blank-collection samples, we dragged the forceps along
624 the petri dish and swirled the forceps inside the original collection tube. We cleaned the tools and petri
625 dish with 70% ethanol and deionized water between individuals and used a new petri dish between
626 sample types. All samples and tubes were kept constantly chilled on dry ice or in liquid nitrogen.

627 **LC-MS/MS processing of ant head samples**: All samples were sent on dry ice to the West
628 Coast Metabolomics Center (WCMC, University of California, Davis) for LC-MS/MS analysis. The
629 WCMC processed samples in three LC-MS/MS protocols broadly tailored toward different chemistries:
630 "biogenic amines," "polyphenols and flavonoids," and "complex lipids." From the 20 samples collected
631 per infection and sham treatments, the WCMC collected polyphenol data for 10 individual ant heads, one
632 from each two-head pool. They used the remaining ten heads per treatment for biphasic extractions, with
633 each individual head used for both biogenic amines and lipids (Fig. 2A). Blank-collection samples were
634 shared across the three LC-MS/MS chemistries. The WCMC produced quality-control (QC) pool samples
635 consisting of all samples used per protocol and additional blank-extraction controls (Fig. 2A). These

636 WCMC control samples were run at the beginning and every ten samples thereafter per protocol. All LC-
637 MS/MS protocols collected MS/MS data in a top-four data-dependent-acquisition (DDA) mode in both
638 electrospray ionization (ESI) positive and negative modes.

639 The WCMC processed samples for biogenic amines for use in hydrophilic interaction
640 chromatography (HILIC) with quadrapole time of flight (Q-TOF) mass spectrometry. Homogenized ant
641 head samples were extracted with a methanol and methyl-tert-butyl ether protocol (Matyash *et al.* 2008)
642 and the aqueous phase used for biogenic amines LC-MS/MS and the organic phase used for lipids (see
643 below). Extractions were mixed with internal standards for normalization according to WCMC protocols
644 to a final volume of 100 µL (Supp. Data 3). Further details are provided in Supp. File 7.

645 Samples for lipids were processed for use in charged surface hybrid (CSH) chromatography with
646 Q-TOF mass spectrometry. The organic phase per biphasic extraction (shared with biogenic amines, see
647 above) was taken for lipids LC-MS/MS and mixed with internal standards according to WCMC protocols
648 (Supp. Data 3) to a final resuspension volume of 110 µL. Further details are provided in Supp. File 7.

649 Samples for polyphenols were processed for use in pentafluorophenyl (PFP) chromatography
650 with QExactive HF (QE) mass spectrometry. Homogenized ant head samples were extracted in a similar
651 fashion as described above and resuspended in a final 100 µL volume with internal standards (Supp. Data
652 3). Further details are provided in Supp. File 7.

653 **Metabolomic data processing & feature filtering:** The WCMC performed initial processing
654 steps on all samples to produce metabolomic feature lists consisting of mass/charge ratio (*m/z*), retention
655 time (rt), and value of quantification ion peaks. They aligned raw data with MS-DIAL (v 4.7.0) (Tsugawa
656 *et al.* 2015), subtracted signals detected in the blank-extractions produced in the core facility, removed
657 duplicate signals and isotopes, normalized samples by internal standards, and assigned compound and
658 adduct annotations based on manual MS/MS matching in Massbank, Metlin, and NIST14 databases and,
659 for lipids, with LipidBlast (v 68) (Kind *et al.* 2013) (Fig. 2B). The resulting data consisted of several
660 thousand features per dataset: biogenic amines (5605 total with 141 annotated), polyphenols (6178 total
661 with 158 annotated), and lipids (7021 with 517 annotated) (Supp. Data 4).

662 We applied additional feature quality control and data reduction methods to create a final list of
663 metabolite features to investigate. Features that had greater than 50% missing values within both sham
664 and infection treatments were removed. Similarly, we removed features with both median peak values
665 (sham and infection) less than double that of median blank-collection peaks. Following removal based on
666 missingness and peak values, we removed features that we determined to have signals too variable for
667 robust analysis based on their coefficient of variation (CV%, or relative standard deviation) (Fig. 2B). For
668 the biogenic amines and lipid datasets that had successful QC pool data returned, we applied a CV%
669 maximum threshold to remove peaks that varied greatly due to technical variation between QC pool
670 injections. We selected the CV% threshold as the lowest (i.e., strictest) value between 30% and a dataset
671 specific value determined from the distribution of CV% values. We calculated this data-specific value as
672 the 75th-quartile + 1.5*interquartile-range (IQR), as is used to identify extreme values or outliers in data
673 distributions (e.g., boxplots). For the lipids, the 1.5*IQR method produced CV 25% as the cutoff,
674 removing 5.7% of features. For biogenic amines, the 1.5*IQR CV% was greater than 30%; therefore,
675 30% was used, removing 6.6% of features. The WCMC reported that all polyphenol QC pools failed on
676 acquisition. Therefore, we ranked each feature by its lowest CV% (i.e., from either CV%-sham or CV%-
677 manipulated) and removed the highest 6.1% of features. We selected this 6.1% value because it was the
678 mean of the CV% removal rates of the biogenic amine and lipid datasets. Although we cannot fully
679 discount biological variation in biogenic amine peak values within a treatment, by selecting the lowest
680 CV% per feature (whether from the sham or infection treatment), we sought to remove only features that
681 had high CV% regardless of treatment. After all these filtering steps, we continued with 3268 biogenic
682 amine features (58% of initially collected), 4878 polyphenol features (79% of initial), and 6305 lipid
683 features (90% of initial).

684 We further applied a putative adduct calling step to consolidate unannotated features that may
685 represent different adducts of the same compound. Per LC-MS/MS dataset, we divided features by
686 treatment and ESI mode, and processed each of these subsets with Binner (v 1.0.0) (Kachman *et al.* 2020)
687 (Fig. 2B). Briefly, Binner compares metabolite features "binned" by rt and calls putative adduct

688 relationships between these features based on a table of possible adducts, feature *m/z*, and correlation of
689 peak values across samples. Data were split by treatment to avoid possibly conflating signals for different
690 compounds found in only one of the treatments as adducts of each other. Data were natural log
691 transformed, no additional deisotoping step was preformed, the mass tolerance was set to 0.005 Da
692 (biogenic amines and lipids) or 0.003 Da (polyphenols), and default settings were used elsewhere. For
693 biogenic amines and polyphenols, we searched for adducts used in KACHMAN *et al.* 2020. For lipids, we
694 supplemented this adduct table with an additional adduct set publicly available online (Fiehn Lab 2020).
695 We then reunited data subsets to create feature lists that included all peaks that were labeled as primary
696 ions or remained unannotated in either treatment group. In effect, this step only removed peaks that were
697 determined to be putative adduct peaks in both treatments, resulting in the final processed datasets for
698 analysis of: 2955 biogenic amines (90% of QC filtered peaks remained), 4315 polyphenols (88% of QC
699 filtered peaks), and 4924 lipids (78% of QC filtered peaks) (Supp. Data 1).

700 **Metabolomic data analysis & feature selection:** To select a single set of study-wide features of
701 interest combined across all three datasets, we applied three statistical approaches (Fig. 2C). For features
702 with values equal to zero, we imputed zeros as 20% of the minimum value measured for that feature.
703 Each analysis we preformed was done independently per LC-MS/MS dataset (biogenic amines, lipids,
704 and polyphenols). We determined if a feature represented a DAM with a t-test (corrected FDR, $p \leq 0.05$)
705 and minimum ±1.5-fold change in abundance between sham and infection treatments. Principal
706 component analyses always indicated that only PC1 separated samples by treatment type (see Results). As
707 such, we noted features ranked in the upper 50% of PC1 absolute loading values. Given that our choice of
708 threshold was defined as half of the data, we did not rely on this test solely as merit for discussing a
709 feature, but rather as a way to add confidence to results of other analyses. Both t-tests and PCAs were
710 performed through the MetaboAnalyst interface (v 5.0) (Pang *et al.* 2021). Finally, we selected features
711 "confirmed" as "important" by Boruta (v 7.0.0, R package) random-forest based analyses with 900
712 maxRuns and 70,000 ntree settings (Kursa and Rudnicki 2010). In brief, "important" features are selected
713 by z-scores of mean decrease accuracy in decision trees in comparison to randomized versions of the data

714 (Kursa and Rudnicki 2010). Boruta offers an improvement over standard random-forest analyses for high
715 dimensional data such as in metabolomics, increasing the stability and robustness of the features selected
716 (Acharjee *et al.* 2020).

717 Additionally, we created co-abundance network modules of metabolite features per LC-MS/MS
718 dataset using the WGCNA method (Langfelder and Horvath 2008) (Fig. 2C). Although the WGCNA was
719 developed primarily for gene expression data, this technique has been used and evaluated for
720 metabolomic data as well (Bartzis *et al.* 2017). Heightened activity in a metabolic pathway could lead to
721 many compounds increasing. But simultaneously, their precursors may become depleted. Therefore,
722 correlations within a network could be both positive and negative. As such, we constructed unsigned
723 WGCNA modules. All WGCNA modules were constructed on feature data without imputing zeros, based
724 on the biweight midcorrelation to compare between treatment types (e.g., corFnc="bicor", robustY=F,
725 maxPOutlier=0.05) (R package WGCNA, v 1.67). In cases where zeros were present, the analysis
726 defaulted to the Pearson correlation for that feature. We obtained similar network modules when the
727 Pearson correlation was used for all features (data not shown). Soft power thresholds were selected
728 according to program recommendations as follows: biogenic amines – 3, polyphenols – 10, and lipids –
729 11.

730 We analyzed different groups of selected features for metabolic pathway enrichments. We formed
731 feature sets that combined data across all three LC-MS/MS datasets based on individual feature selection
732 analyses (t-test, PCA, and Boruta) or their presence only in manipulation samples. Dataset-specific
733 network modules were only analyzed with background features from the LC-MS/MS dataset they
734 belonged to and if the module was correlated to treatment (Student correlation $\geq |0.5|$, $p \leq 0.05$) (Fig. 2C).

735 We preformed Mummichog analyses on these feature sets (Li *et al.* 2013), as described in Results
736 & Discussion. This process matched 1,523 unique metabolite features to 6,725 KEGG annotated
737 compounds. For enrichment analyses combining features across datasets, we additionally used a
738 technique based on GSEA ranking features by t-scores returned by t-tests (Subramanian *et al.* 2005). In
739 network module pathway enrichment analyses, only Mummichog was used as it sets a hard threshold to

740 define a group of interest versus the background. Membership within or out of a network module was
741 simply defined and could be used for this division. All enrichment analyses were conducted through the
742 MetaboAnalyst interface with the following settings: Mixed ion mode, 3 ppm mass tolerance, retention
743 time included, primary ions not enforced, all adducts tested, default currency metabolites, and conducted
744 once for both the *Drosophila melanogaster* and *Saccharomyces cerevisiae* KEGG metabolic pathway and
745 compound databases (Fig. 2C). As we sought to characterize the composite metabolome of manipulated
746 ant heads containing both insect and fungal tissue, we chose both a well-studied insect and fungal model
747 organism to improve our odds of matching annotations. We did not use results from one database or the
748 other to discriminate between a host (ant) or parasite (fungus) signal. Neither of the databases would
749 represent the full metabolic repertoire of their respective model organisms and combining them could
750 offer more complete data for comparison. Furthermore, we wished to consider the possibility that due to
751 the relationship of the host and parasite, either organism may be producing metabolites canonically
752 associated with the other as part of its strategy in this antagonism.

753 We selected significantly enriched pathways based on one of the hypergeometric enrichment
754 results reported by MetaboAnalyst. When using Mummichog only (WGCNA module feature set), we
755 used the gamma-null adjusted p-value (≤ 0.05). When including a GSEA as a joint analysis (study-wide
756 feature set), we used the combined p-value (≤ 0.05), calculated with MetaboAnalyst using the Fisher
757 method. Of the overrepresented pathways selected by the enrichment analyses ($p \leq 0.05$), we further
758 imposed thresholds for: (*i*) a minimum of three selected features in the pathway, (*ii*) 1.25-fold enrichment,
759 and (*iii*) three DEGs (see below) encoding associated enzymes to discard weak signals that would likely
760 be difficult to interpret biologically in a multiomic pathway-level context (Fig. 2C). For cases when a
761 pathway was selected using both *D. melanogaster* and *S. cerevisiae* KEGG databases, a mean p-value and
762 fold-enrichment is reported.

763 **Multiomics integration of genomic and transcriptomic data:** We interpreted results of this
764 work's LC-MS/MS data in light of previously collected transcriptomic RNAseq data when possible (Will
765 *et al.* 2020). That RNAseq data was collected with a similar experimental framework, including

766 comparisons of gene expression of both *C. floridanus* and *O. camponoti-floridani* between a control
767 (uninfected ant or fungal culture) and manipulated ant samples. Identification of DEGs (Cuffdiff analysis
768 corrected FDR $p \leq 0.05$, minimum two-fold change, minimum 4 RPKM) and relevant statistics are
769 reported in Will *et al.* 2020. For each enriched metabolic pathway, we retrieved gene sequence data for
770 enzymes associated with that pathway in KEGG (by enzyme nomenclature EC number). For each enzyme
771 EC, we extracted the first representative gene listed for *D. melanogaster* and *S. cerevisiae*. We searched
772 for reciprocal best matches to those genes in both the *C. floridanus* and *O. camponoti-floridani* genomes
773 using Proteinortho (v 5) with default settings (Lechner *et al.* 2011). While this non-exhaustive approach
774 would not identify every possible *C. floridanus* or *O. camponoti-floridani* gene with homology to known
775 enzymes of interest, it did assist with initially selecting pathway enrichments for deeper analysis. Per
776 pathway, we required that at least three DEGs combined from both transcriptomes of the ant and fungus
777 had homologs to the enzymes associated with that pathway. This selection criterion followed the
778 pathway-level thinking to require at least three contributing metabolite features matched by Mummichog
779 to consider an enrichment result for discussion. Metabolic pathway relationships were based on KEGG
780 data and supplemented by other sources where cited.
781
782 **Data Availability**
783 Genomic and transcriptomic data referenced here are available in Will *et al.* 2020 and the
784 GenBank accessions reported therein. Supplemental Data files (Supp. Data 1-4) are available upon
785 request while at the preprint stage.
786
787 **Acknowledgments**
788 We would like to thank Sophia Vermeulen for assisting with testing fungal strain OJ2.1 and, with
789 Biplabendu Das, their help with ant infections and observations. We also thank Devin Burris for help with
790 ant monitoring. Jordan Dowell provided insightful discussions on LC-MS/MS methods and interpretation
791 for which we are grateful for. The Genetics Society of America provided travel support for dissemination

of early results of this work. Research funding for this project came from NSF (NSF-CAREER IOS-1941546 awarded to C.dB).

795 **References**

796 Acharjee, A., J. Larkman, Y. Xu, V. R. Cardoso, and G. V. Gkoutos, 2020 A random forest based
797 biomarker discovery and power analysis framework for diagnostics research. BMC Med. Genomics
798 13: 1–14.

799 Adamo, S. A., 2008 Norepinephrine and octopamine: linking stress and immune function across phyla.
800 ISJ 5: 12–19.

801 Adamo, S. A., 2019 Turning your victim into a collaborator: exploitation of insect behavioral control
802 systems by parasitic manipulators. Curr. Opin. Insect Sci. 33: 25–29.

803 Adamo, S. A., C. E. Linn, and N. E. Beckage, 2013 Parasites: evolution's neurobiologists. J. Exp. Biol.
804 216: 3–10.

805 Alecu, I., and S. A. L. Bennett, 2019 Dysregulated lipid metabolism and its role in α-synucleinopathy in
806 Parkinson's disease. Front. Neurosci. 13: 328.

807 Andersen, S. B., S. Gerritsma, K. M. Yusah, D. Mayntz, N. L. Hywel-Jones *et al.*, 2009 The Life of a
808 Dead Ant: The Expression of an Adaptive Extended Phenotype. Am. Nat. 174: 424–433.

809 Andriolli, F. S., N. K. Ishikawa, R. Vargas-Isla, T. S. Cabral, C. de Bekker *et al.*, 2019 Do zombie ant
810 fungi turn their hosts into light seekers? Behav. Ecol. 30: 609–616.

811 Aonuma, H., 2020 Serotonergic control in initiating defensive responses to unexpected tactile stimuli in
812 the trap-jaw ant Odontomachus kuroiwae. J. Exp. Biol. 223:.

813 Aonuma, H., and T. Watanabe, 2012 Changes in the content of brain biogenic amine associated with early
814 colony establishment in the Queen of the ant, Formica japonica. PLoS One 7: e43377–e43377.

815 Bartzis, G., J. Deelen, J. Maia, W. Ligterink, H. W. M. Hilhorst *et al.*, 2017 Estimation of metabolite
816 networks with regard to a specific covariable: applications to plant and human data. Metabolomics
817 13: 129.

818 Batrakov, S. G., I. V. Konova, V. I. Sheichenko, S. E. Esipov, and L. A. Galanina, 2001 Two unusual
819 glycerophospholipids from a filamentous fungus, Absidia corymbifera. Biochim. Biophys. Acta -
820 Mol. Cell Biol. Lipids 1531: 169–177.

821 de Bekker, C., 2019 Ophiocordyceps–ant interactions as an integrative model to understand the molecular
822 basis of parasitic behavioral manipulation. Curr. Opin. Insect Sci. 33: 19–24.
823 de Bekker, C., W. C. Beckerson, and C. Elya, 2021 Mechanisms behind the Madness: How Do Zombie-
824 Making Fungal Entomopathogens Affect Host Behavior To Increase Transmission? (D. A. Garsin,
825 Ed.). MBio.
826 de Bekker, C., and B. Das, 2022 Hijacking time: How Ophiocordyceps fungi could be using ant host
827 clocks to manipulate behavior. Parasite Immunol. 44: e12909.
828 de Bekker, C., M. Merrow, and D. P. Hughes, 2014a From behavior to mechanisms: An integrative
829 approach to the manipulation by a parasitic fungus (Ophiocordyceps unilateralis s.l.) of its host ants
830 (Camponotus spp.). Integr. Comp. Biol. 52: 166–176.
831 de Bekker, C., R. A. Ohm, R. G. Loreto, A. Sebastian, I. Albert *et al.*, 2015 Gene expression during
832 zombie ant biting behavior reflects the complexity underlying fungal parasitic behavioral
833 manipulation. BMC Genomics 16: 620.
834 de Bekker, C., L. E. Quevillon, P. B. Smith, K. R. Fleming, D. Ghosh *et al.*, 2014b Species-specific Ant
835 Brain Manipulation by a Specialized Fungal Parasite. BMC Evol. Biol. 14: 166.
836 Boulay, R., V. Soroker, E. J. Godzinska, A. Hefetz, and A. Lenoir, 2000 Octopamine reverses the
837 isolation-induced increase introphallaxis in the carpenter ant Camponotus Fellah. Journgal Exp.
838 Biol. 203: 513–520.
839 Carlson, M. R. J., B. Zhang, Z. Fang, P. S. Mischel, S. Horvath *et al.*, 2006 Gene connectivity, function,
840 and sequence conservation: Predictions from modular yeast co-expression networks. BMC
841 Genomics 7: 1–15.
842 Cassilly, C. D., and T. B. Reynolds, 2018 PS, It's Complicated: The Roles of Phosphatidylserine and
843 Phosphatidylethanolamine in the Pathogenesis of Candida albicans and Other Microbial Pathogens.
844 J. Fungi 4:.
845 Coleman, C. M., and W. S. Neckameyer, 2005 Serotonin synthesis by two distinct enzymes in Drosophila
846 melanogaster. Arch. Insect Biochem. Physiol. 59: 12–31.

847 Colovic, M. B., D. Z. Krstic, T. D. Lazarevic-Pasti, A. M. Bondzic, and V. M. Vasic, 2013
848 Acetylcholinesterase Inhibitors: Pharmacology and Toxicology. Curr. Neuropharmacol. 11: 315.
849 Dakshinamurti, K., S. Dakshinamurti, M. P. Czubryt, K. Dakshinamurti, S. Dakshinamurti *et al.*, 2017
850 Vitamin B6: Effects of Deficiency, and Metabolic and Therapeutic Functions. Handb. Famine,
851 Starvation, Nutr. Deprivation 1–23.
852 Dawaliby, R., C. Trubbia, C. Delporte, C. Noyon, J. M. Ruysschaert *et al.*, 2016
853 Phosphatidylethanolamine Is a Key Regulator of Membrane Fluidity in Eukaryotic Cells. J. Biol.
854 Chem. 291: 3658.
855 Diez, L., P. Lejeune, and C. Detrain, 2014 Keep the nest clean: survival advantages of corpse removal in
856 ants. Biol. Lett. 10:.
857 Feng, P., Y. Shang, K. Cen, and C. Wang, 2015 Fungal biosynthesis of the bibenzoquinone oosporein to
858 evade insect immunity. Proc. Natl. Acad. Sci. U. S. A. 112: 11365–11370.
859 Fiehn Lab, 2020 ESI-MS-adducts-2020.
860 Fournier, D., J.-M. Bride, F. Hoffmann, and F. Karch, 1992 Acetylcholinesterase TWO TYPES OF
861 MODIFICATIONS CONFER RESISTANCE TO INSECTICIDE. J. Biol. Chem. 267: 14270–
862 14274.
863 Fredericksen, M. A., Y. Zhang, M. L. Hazen, R. G. Loreto, C. A. Mangold *et al.*, 2017 Three-dimensional
864 visualization and a deep-learning model reveal complex fungal parasite networks in behaviorally
865 manipulated ants. Proc. Natl. Acad. Sci. 114: 201711673.
866 Friedman, D. A., A. Pilko, D. Skowronska-Krawczyk, K. Krasinska, J. W. Parker *et al.*, 2018 The Role of
867 Dopamine in the Collective Regulation of Foraging in Harvester Ants. iScience 8: 283.
868 Gasparetti, C., E. Nordlund, J. Jänis, J. Buchert, and K. Kruus, 2012 Extracellular tyrosinase from the
869 fungus Trichoderma reesei shows product inhibition and different inhibition mechanism from the
870 intracellular tyrosinase from Agaricus bisporus. Biochim. Biophys. Acta - Proteins Proteomics
871 1824: 598–607.
872 Gauthier, M., 2010 *Insect Nicotinic Acetylcholine Receptors: State of the Art on Insect Nicotinic*

873 *Acetylcholine Receptor Function in Learning and Memory* (S. Hervé Thany, Ed.).
874 Geun, S. K., M. Nalini, Y. Kim, and D. W. Lee, 2009 Octopamine and 5-hydroxytryptamine mediate
875 hemocytic phagocytosis and nodule formation via eicosanoids in the beet armyworm, Spodoptera
876 exigua. Arch. Insect Biochem. Physiol. 70: 162–176.
877 Gillis, J., and P. Pavlidis, 2012 "Guilt by Association" Is the Exception Rather Than the Rule in Gene
878 Networks. PLOS Comput. Biol. 8: e1002444.
879 González-Santoyo, I., and A. Córdoba-Aguilar, 2012 Phenoloxidase: a key component of the insect
880 immune system. Entomol. Exp. Appl. 142: 1–16.
881 Gorman, M. J., and Y. Arakane, 2010 Tyrosine hydroxylase is required for cuticle sclerotization and
882 pigmentation in Tribolium castaneum. Insect Biochem. Mol. Biol. 40: 267–273.
883 Grünewald, B., and P. Siefert, 2019 Acetylcholine and Its Receptors in Honeybees: Involvement in
884 Development and Impairments by Neonicotinoids. Insects 10:.
885 Heil, M., 2016 Host Manipulation by Parasites: Cases, Patterns, and Remaining Doubts. Front. Ecol.
886 Evol. 4: 80.
887 Helluy, S., 2013 Parasite-induced alterations of sensorimotor pathways in gammarids: collateral damage
888 of neuroinflammation? J. Exp. Biol. 216: 67–77.
889 Helluy, S., and J. C. Holmes, 1990 Serotonin, octopamine, and the clinging behavior induced by the
890 parasite Polymorphus paradoxus (Acanthocephala) in Gammarus lacustris (Crustacea). Can. J. Zool.
891 68: 1214–1220.
892 Herbison, R. E. H., 2017 Lessons in Mind Control: Trends in Research on the Molecular Mechanisms
893 behind Parasite-Host Behavioral Manipulation. Front. Ecol. Evol. 5: 102.
894 Hoxmeier, J. C., B. D. Thompson, C. D. Broeckling, P. Small, B. D. Foy *et al.*, 2015 Analysis of the
895 metabolome of Anopheles gambiae mosquito after exposure to Mycobacterium ulcerans. Sci.
896 Reports 2015 51 5: 1–8.
897 Hughes, D. P., S. B. Andersen, N. L. Hywel-Jones, W. Himaman, J. Billen *et al.*, 2011 Behavioral
898 mechanisms and morphological symptoms of zombie ants dying from fungal infection. BMC Ecol.

899 11: 13.
900 Johansen, J., M. E. Halpern, K. M. Johansen, and H. Keshishian, 1989 Stereotypic morphology of
901 glutamatergic synapses on identified muscle cells of Drosophila larvae. J. Neurosci. 9: 710.
902 Kachman, M., H. Habra, W. Duren, J. Wigginton, P. Sajjakulnukit *et al.*, 2020 Deep annotation of
903 untargeted LC-MS metabolomics data with Binner. Bioinformatics 36: 1801–1806.
904 Kamhi, J. F., S. Arganda, C. S. Moreau, and J. F. A. Traniello, 2017 Origins of aminergic regulation of
905 behavior in complex insect social systems. Front. Syst. Neurosci. 11: 74.
906 Kanehisa, M., and S. Goto, 2000 KEGG: Kyoto Encyclopedia of Genes and Genomes. Nucleic Acids
907 Res. 28: 27.
908 Kassambara, A., M. Kosinski, P. Biecek, and S. Fabian, 2019 Drawing Survival Curves using "ggplot2"
909 [R package survminer version 0.4.4].
910 Kim, Y. H., and S. H. Lee, 2013 Which acetylcholinesterase functions as the main catalytic enzyme in the
911 Class Insecta? Insect Biochem. Mol. Biol. 43: 47–53.
912 Kind, T., K. H. Liu, D. Y. Lee, B. Defelice, J. K. Meissen *et al.*, 2013 LipidBlast in silico tandem mass
913 spectrometry database for lipid identification. Nat. Methods 2013 108 10: 755–758.
914 Kobmoo, N., D. Wichadakul, N. Arnamnart, R. C. Rodríguez De La Vega, J.-J. J. Luangsa-ard *et al.*,
915 2018 A genome scan of diversifying selection in Ophiocordyceps zombie-ant fungi suggests a role
916 for enterotoxins in co-evolution and host specificity. Mol. Ecol. 27: 3582–3598.
917 Kursa, M. B., and W. R. Rudnicki, 2010 Feature Selection with the Boruta Package. J. Stat. Softw. 36: 1–
918 13.
919 Lafferty, K. D., and J. C. Shaw, 2013 Comparing mechanisms of host manipulation across host and
920 parasite taxa. J. Exp. Biol. 216: 56–66.
921 Langfelder, P., and S. Horvath, 2008 WGCNA: an R package for weighted correlation network analysis.
922 BMC Bioinformatics 9: 559.
923 Leboeuf, A. C., P. Waridel, C. S. Brent, A. N. Gonçalves, L. Menin *et al.*, 2016 Oral transfer of chemical
924 cues, growth proteins and hormones in social insects. Elife 5:.

925 Lechner, M., S. Findeiß, L. Steiner, M. Marz, P. F. Stadler *et al.*, 2011 Proteinortho: Detection of (Co-
926)orthologs in large-scale analysis. BMC Bioinformatics 12: 1–9.
927 Lee, Y. S., Y. S. Park, S. Nam, S. J. Suh, J. Lee *et al.*, 2000 Characterization of GAR-2, a Novel G
928 Protein-Linked Acetylcholine Receptor from Caenorhabditis elegans. J. Neurochem. 75: 1800–1809.
929 Lefèvre, T., S. A. Adamo, D. G. Biron, D. Missé, D. Hughes *et al.*, 2009 Invasion of the body snatchers:
930 the diversity and evolution of manipulative strategies in host-parasite interactions. Adv. Parasitol.
931 68: 45–83.
932 Li, S., Y. Park, S. Duraisingham, F. H. Strobel, N. Khan *et al.*, 2013 Predicting Network Activity from
933 High Throughput Metabolomics. PLOS Comput. Biol. 9: e1003123.
934 Li, Z., and D. E. Vance, 2008 Thematic Review Series: Glycerolipids. Phosphatidylcholine and choline
935 homeostasis. J. Lipid Res. 49: 1187–1194.
936 Libersat, F., M. Kaiser, and S. Emanuel, 2018 Mind Control: How Parasites Manipulate Cognitive
937 Functions in Their Insect Hosts. Front. Psychol. 9: 572.
938 Loreto, R. G., J. P. M. Araújo, R. M. Kepler, K. R. Fleming, C. S. Moreau *et al.*, 2018 Evidence for
939 convergent evolution of host parasitic manipulation in response to environmental conditions.
940 Evolution (N. Y). 211144.
941 Loreto, R. G., and D. P. Hughes, 2019 The metabolic alteration and apparent preservation of the zombie
942 ant brain. J. Insect Physiol. 118: 103918.
943 Lovett, B., R. J. St. Leger, and H. H. de Fine Licht, 2020 Going gentle into that pathogen-induced
944 goodnight. J. Invertebr. Pathol. 174: 107398.
945 Mangold, C. A., M. J. Ishler, R. G. Loreto, M. L. Hazen, and D. P. Hughes, 2019 Zombie ant death grip
946 due to hypercontracted mandibular muscles. J. Exp. Biol. 222: jeb200683.
947 Matyash, V., G. Liebisch, T. V. Kurzchalia, A. Shevchenko, and D. Schwudke, 2008 Lipid extraction by
948 methyl-tert-butyl ether for high-throughput lipidomics. J. Lipid Res. 49: 1137–1146.
949 Moore, J., 2013 An overview of parasite-induced behavioral alterations - and some lessons from bats. J.
950 Exp. Biol. 216: 11–7.

951 Muscedere, M. L., N. Johnson, B. C. Gillis, J. F. Kamhi, and J. F. A. Traniello, 2012 Serotonin modulates
952 worker responsiveness to trail pheromone in the ant Pheidole dentata. J. Comp. Physiol. A
953 Neuroethol. Sensory, Neural, Behav. Physiol. 198: 219–227.
954 Neckameyer, W. S., C. M. Coleman, S. Eadie, and S. F. Goodwin, 2007 Compartmentalization of
955 neuronal and peripheral serotonin synthesis in Drosophila melanogaster. Genes, Brain Behav. 6:
956 756–769.
957 Neckameyer, W. S., and K. White, 1992 A single locus encodes both phenylalanine hydroxylase and
958 tryptophan hydroxylase activities in Drosophila. J. Biol. Chem. 267: 4199–4206.
959 Nosanchuk, J. D., and A. Casadevall, 2006 Impact of melanin on microbial virulence and clinical
960 resistance to antimicrobial compounds. Antimicrob. Agents Chemother. 50: 3519–3528.
961 Nosanchuk, J. D., R. E. Stark, and A. Casadevall, 2015 Fungal melanin: What do we know about
962 structure? Front. Microbiol. 6: 1463.
963 Pang, Z., J. Chong, G. Zhou, D. A. De Lima Morais, L. Chang *et al.*, 2021 MetaboAnalyst 5.0: narrowing
964 the gap between raw spectra and functional insights. Nucleic Acids Res. 49: W388–W396.
965 Pflüger, H. J., and C. Duch, 2011 Dynamic neural control of insect muscle metabolism related to motor
966 behavior. Physiology 26: 293–303.
967 Piao, S., Y. L. Song, H. K. Jung, Y. P. Sam, W. P. Ji *et al.*, 2005 Crystal structure of a clip-domain serine
968 protease and functional roles of the clip domains. EMBO J. 24: 4404.
969 Pokotylo, I., P. Pejchar, M. Potocký, D. Kocourková, Z. Krčková *et al.*, 2013 The plant non-specific
970 phospholipase C gene family. Novel competitors in lipid signalling. Prog. Lipid Res. 52: 62–79.
971 Pontoppidan, M. B., W. Himaman, N. L. Hywel-Jones, J. J. Boomsma, and D. P. Hughes, 2009
972 Graveyards on the move: The spatio-temporal distribution of dead ophiocordyceps-infected ants (A.
973 Dornhaus, Ed.). PLoS One 4: e4835.
974 Prandovszky, E., E. Gaskell, H. Martin, J. P. Dubey, J. P. Webster *et al.*, 2011 The Neurotropic Parasite
975 Toxoplasma Gondii Increases Dopamine Metabolism. PLoS One 6: e23866.
976 Quinn, D. M., 1987 Acetylcholinesterase: Enzyme Structure, Reaction Dynamics, and Virtual Transition

977 States. Chem. Reiviews 87: 955–979.
978 R Core Team, 2021 R: A language and environment for statistical computing.
979 Ramirez, J. L., E. J. Muturi, C. Dunlap, and A. P. Rooney, 2018 Strain-specific pathogenicity and
980 subversion of phenoloxidase activity in the mosquito Aedes aegypti by members of the fungal
981 entomopathogenic genus Isaria. Sci. Reports 2018 81 8: 1–12.
982 RStudio Team, 2015 RStudio: Integrated Development for R.
983 Sakolrak, B., R. Blatrix, U. Sangwanit, and N. Kobmoo, 2018 Experimental infection of the ant
984 Polyrhachis furcata with Ophiocordyceps reveals specificity of behavioural manipulation. Fungal
985 Ecol. 33: 122–124.
986 Selinheimo, E., M. Saloheimo, E. Ahola, A. Westerholm-Parvinen, N. Kalkkinen *et al.*, 2006 Production
987 and characterization of a secreted, C-terminally processed tyrosinase from the filamentous fungus
988 Trichoderma reesei. FEBS J. 273: 4322–4335.
989 Shaw, J. C., W. J. Korzan, R. E. Carpenter, A. M. Kuris, K. D. Lafferty *et al.*, 2009 Parasite manipulation
990 of brain monoamines in California killifish (Fundulus parvipinnis) by the trematode Euhaplorchis
991 californiensis. Proc. R. Soc. B Biol. Sci. 276: 1137–1146.
992 Shyu, P., B. S. H. Ng, N. Ho, R. Chaw, Y. L. Seah *et al.*, 2019 Membrane phospholipid alteration causes
993 chronic ER stress through early degradation of homeostatic ER-resident proteins. Sci. Reports 2019
994 91 9: 1–15.
995 Singh, K. D., R. K. Labala, T. B. Devi, N. I. Singh, H. D. Chanu *et al.*, 2017 Biochemical efficacy,
996 molecular docking and inhibitory effect of 2, 3-dimethylmaleic anhydride on insect
997 acetylcholinesterase. Sci. Reports 2017 71 7: 1–11.
998 Stuart, J. M., E. Segal, D. Koller, and S. K. Kim, 2003 A gene-coexpression network for global discovery
999 of conserved genetic modules. Science (80-.). 302: 249–255.
1000 Subramanian, A., P. Tamayo, V. K. Mootha, S. Mukherjee, B. L. Ebert *et al.*, 2005 Gene set enrichment
1001 analysis: A knowledge-based approach for interpreting genome-wide expression profiles. Proc. Natl.
1002 Acad. Sci. U. S. A. 102: 15545–15550.

1003 Sugumaran, M., and H. Barek, 2016 Critical Analysis of the Melanogenic Pathway in Insects and Higher
1004 Animals. Int. J. Mol. Sci. 17:.
1005 Szczuka, A., J. Korczyńska, A. Wnuk, B. Symonowicz, A. Gonzalez Szwacka *et al.*, 2013 The effects of
1006 serotonin, dopamine, octopamine and tyramine on behavior of workers of the ant Formica polyctena
1007 during dyadic aggression tests. Acta Neurobiol. Exp. (Wars). 73: 495–520.
1008 Therneau, T., 2015 A Package for Survival Analysis in S.
1009 Thomas, F., R. Poulin, and J. Brodeur, 2010 Host manipulation by parasites: A multidimensional
1010 phenomenon. Oikos 119: 1217–1223.
1011 Trinh, T., R. Ouellette, and C. de Bekker, 2021 Getting lost: the fungal hijacking of ant foraging
1012 behaviour in space and time. Anim. Behav. 181: 165–184.
1013 Tsugawa, H., T. Cajka, T. Kind, Y. Ma, B. Higgins *et al.*, 2015 MS-DIAL: data-independent MS/MS
1014 deconvolution for comprehensive metabolome analysis. Nat. Methods 2015 126 12: 523–526.
1015 VanderMolen, K. M., H. A. Raja, T. El-Elimat, and N. H. Oberlies, 2013 Evaluation of culture media for
1016 the production of secondary metabolites in a natural products screening program. AMB Express 3:
1017 71.
1018 van der Veen, J. N., J. P. Kennelly, S. Wan, J. E. Vance, D. E. Vance *et al.*, 2017 The critical role of
1019 phosphatidylcholine and phosphatidylethanolamine metabolism in health and disease. Biochim.
1020 Biophys. Acta - Biomembr. 1859: 1558–1572.
1021 Verlinden, H., 2018 Dopamine signalling in locusts and other insects. Insect Biochem. Mol. Biol. 97: 40–
1022 52.
1023 Walter, A., U. Korth, M. Hilgert, J. Hartmann, O. Weichel *et al.*, 2004 Glycerophosphocholine is elevated
1024 in cerebrospinal fluid of Alzheimer patients. Neurobiol. Aging 25: 1299–1303.
1025 Wang, Y., H. Jiang, Y. Cheng, C. An, Y. Chu *et al.*, 2017 Activation of Aedes aegypti prophenoloxidase-
1026 3 and its role in the immune response against entomopathogenic fungus. Insect Mol. Biol. 26: 552.
1027 Will, I., W. C. Beckerson, and C. de Bekker, 2022a Using machine learning to predict protein-protein
1028 interactions between a zombie ant fungus and its carpenter ant host. bioRxiv 2022.09.09.507359.

1029 Will, I., B. Das, T. Trinh, A. Brachmann, R. A. Ohm *et al.*, 2020 Genetic Underpinnings of Host
1030 Manipulation by Ophiocordyceps as Revealed by Comparative Transcriptomics. G3 (Bethesda). 10:
1031 2275–2296.
1032 Will, I., S. Linehan, D. G. Jenkins, and C. de Bekker, 2022b Natural history and ecological effects on the
1033 establishment and fate of Florida carpenter ant cadavers infected by the parasitic manipulator
1034 Ophiocordyceps camponoti-floridani. Funct. Ecol. 00: 1–14.
1035 Yakovlev, I. K., 2018 Effects of Octopamine on Aggressive Behavior in Red Wood Ants. Neurosci.
1036 Behav. Physiol. 2018 483 48: 279–288.
1037 Zheng, S., R. Loreto, P. Smith, A. Patterson, D. Hughes *et al.*, 2019 Specialist and Generalist Fungal
1038 Parasites Induce Distinct Biochemical Changes in the Mandible Muscles of Their Host. Int. J. Mol.
1039 Sci. 20:.
1040 Zhuang, J. X., Y. H. Hu, M. H. Yang, F. J. Liu, L. Qiu *et al.*, 2010 Irreversible Competitive Inhibitory
1041 Kinetics of Cardol Triene on Mushroom Tyrosinase. J. Agric. Food Chem. 58: 12993–12998.
1042